Comenius University in Bratislava
Faculty of Mathematics, Physics and Informatics

Flow polynomials of k-poles

Master's Thesis

2024
Bc. Dávid Mišiak

Comenius University in Bratislava
Faculty of Mathematics, Physics and Informatics

Flow polynomials of k-poles

Master's Thesis

Study Programme:	Computer Science
Field of Study:	Computer Science
Department:	Department of Computer Science
Supervisor:	doc. RNDr. Robert Lukoťka, PhD.

Bratislava, 2024
Bc. Dávid Mišiak

Univerzita Komenského v Bratislave
Fakulta matematiky, fyziky a informatiky

ZADANIE ZÁVEREČNEJ PRÁCE

Meno a priezvisko študenta: Bc. Dávid Mišiak
Študijný program: informatika (Jednoodborové štúdium, magisterský II. st., denná forma)
Študijný odbor: informatika
Typ záverečnej práce: diplomová
Jazyk záverečnej práce: anglický
Sekundárny jazyk: slovenský

Názov: Flow polynomials of k-poles
Tokové polynómy k-pólov

Anotácia: k-pól je pár (G, T), kde G je graf a T je k-tica rôznych vrcholov stupňa jedna v G. Nech H je ábelovská grupa. H-reťazec v (G, T) je priradenie orientácie a nenulových hodnôt H hranám G. Hranica vrchola v je rozdiel medzi súčtom hodnôt na hranách vchádzajúcich do v a súčtom hodnôt na hranách vychádzajúcich z v. H-tok je H-reťazec ktorého hranica je 0 pre všetky vrcholy, ktoré nie sú v T. Ak máme daný H-tok phi k-pólu (G, T), hranicou phi je k-tica, ktorej i-ty prvok je hranica i-teho vrchola T v phi.
Enumerovanie počtu tokov n na danom k-póle s danou hranicou možno dosiahnuť pomocou rekurzívneho vzorca n(G) = n(G/e) - n(G-e). Toto ukazuje, že pre danú grupu H počet tokov (G, T) s danou hranicou možno vyjadriť ako lineárny polynóm, ktorého koeficienty reprezentujú grafy bez vnútorných hrán (pozri napr. [M. Kochol: Restrictions On Smallest Counterexamples To The 5-Flow Conjecture, Combinatorica 26 (2006)].
Cieľom práce je študovať vlastnosti týchto polynómov pre H=Z_2xZ_2 s dôrazom na planárny prípad.

Vedúci: doc. RNDr. Robert Lukoťka, PhD.
Katedra: FMFI.KI - Katedra informatiky
Vedúci katedry: prof. RNDr. Martin Škoviera, PhD.

Spôsob sprístupnenia elektronickej verzie práce:
bez obmedzenia

Dátum zadania: 06.10.2022

Dátum schválenia: 28.04.2023 prof. RNDr. Rastislav Kráľovič, PhD.
garant študijného programu

.....
študent

.....
vedúci práce

Comenius University Bratislava
Faculty of Mathematics, Physics and Informatics

THESIS ASSIGNMENT

Name and Surname:	Bc. Dávid Mišiak
Study programme:	Computer Science (Single degree study, master II. deg., full time form)
Field of Study:	Computer Science
Type of Thesis:	Diploma Thesis
Language of Thesis:	English
Secondary language:	Slovak

Title: Flow polynomials of k-poles

Annotation: A k-pole is a pair (G, T), where G is a graph and T is a k-tuple of distinct vertices that have degree one in G. Let H be an abelian group. An H-chain on (G, T) is an assignment of an orientation and non-zero elements of H to the edges of G. The boundary of a vertex v in an H-chain phi is the sum of values of edges incoming to v minus the sum of values outgoing from v. An H-flow is a chain that has boundary 0 for each vertex of G that is not in T. Given an H-flow phi of (G, T) the boundary of phi is the tuple whose i-th element equals boundary of i-th element of T in phi.
To enumerate number of flows n(G) on given k-pole with given boundary one can use recursive formula n(G) = n(G/e) - n(G-e). This shows that for a fixed group H the number of flows with given boundary can be expressed as a linear polynomial whose coefficients are k-poles with no internal edges (see e.g. [M. Kochol: Restrictions On Smallest Counterexamples To The 5-Flow Conjecture, Combinatorica 26 (2006)].
The aim of the thesis is to study properties of these polynomials for H=Z_2xZ_2 with emphasis on the planar case.

Supervisor:	doc. RNDr. Robert Lukoťka, PhD.
Department:	FMFI.KI - Department of Computer Science
Head of department:	prof. RNDr. Martin Škoviera, PhD.
Assigned:	06.10.2022
Approved:	28.04.2023

prof. RNDr. Rastislav Kráľovič, PhD.
Guarantor of Study Programme

.....
Student

.....
Supervisor

Acknowledgments: I want to thank my supervisor doc. RNDr. Robert Lukoťka, PhD. for his guidance and consistent support throughout the work on this thesis.

Abstrakt

Veta o štyroch farbách sa dá preformulovať na problém hľadania tokov nad grupou $(\mathbb{Z}_2 \times \mathbb{Z}_2, +)$ v kubických planárnych grafoch. Pre multipóly (grafy s trčiacimi hranami) je s využitím rekurzívneho vzťahu pre tokový polynóm možné vyjadriť počet tokov ako lineárnu kombináciu počtov tokov v malých, základných multipóloch. V práci skúmame vlastnosti planárnych multipólov z hľadiska koeficientov tohto výrazu. Venujeme sa najmä multipólovej súvislosti a počtom tokov s danou hranicou; tieto vlastnosti úzko súvisia s Vetou o štyroch farbách. V práci tiež prezentujeme algoritmus na výpočet koeficientov a výsledky výpočtov na kubických planárnych multipóloch do približne 30 vrcholov. Na základe týchto výsledkov odpozorujeme a vyslovíme hypotézu o hranových 3-farbeniach kubických planárnych 5-pólov: Aspoň štvrtina všetkých farbení každého 5-pólu má tri po sebe idúce trčiace hrany rovnakej farby. Napokon skúmame vlastnosti prípadného protipríkladu k tejto hypotéze.

Kľúčové slová: multipól, tokový polynóm, planárny graf, Veta o štyroch farbách

Abstract

The Four color theorem can be reformulated as the problem of finding flows over the group $(\mathbb{Z}_2 \times \mathbb{Z}_2, +)$ in cubic planar graphs. Using the recursive relation for the flow polynomial, it is possible to express the number of flows in a multipole (a graph with dangling edges) as a linear combination of flow counts in small, basic multipoles. In this thesis, we study the properties of planar multipoles from the perspective of the coefficients in this expression. We focus on multipole connectivity and the number of flows with given boundary values; these properties are closely related to the Four color theorem. We also present an algorithm for computing the coefficients and the results of computations on cubic planar multipoles up to approximately 30 vertices. Based on these results, we observe and formulate a hypothesis about 3-edge-colorings of cubic planar 5-poles: At least one-quarter of all colorings of each 5-pole contain three consecutive dangling edges of the same color. Finally, we investigate the properties of a potential counterexample to this hypothesis.

Keywords: multipole, flow polynomial, planar graph, Four color theorem

Contents

List of Figures

List of Tables

Introduction

Among the vast field of graph theory, the Four color theorem is one of the most famous and intriguing results. Although proven, there is still much to be studied about the properties of planar graphs and their colorings. One could even speculate about different, not yet discovered approaches to proving the theorem. The aim of this thesis is to study one of such potentially interesting devices.

In the first chapter, we introduce the most important concepts related to our work. We present the *multipole polynomial*—the central idea that our work builds upon: the number of flows expressed as a linear combination of the flow counts in basic multipoles. We establish the necessary terminology and show a motivational example that illustrates the utility of the multipole polynomial coefficients.

In the second chapter, we exhibit the effectiveness of the coefficients in capturing information about the flow counts with given boundary values in a multipole. The focus of the third chapter is on determining the relationship between coefficient values and the connectivity properties of multipoles.

To learn more about the empirical values of the coefficients, we present a trivial as well as an advanced algorithm for computing them in the fourth chapter. We briefly describe some of the interesting implementation aspects. Thanks to the computation being efficient in practice, we analyze the computed values in the fifth chapter. We compare the theoretical constraints on the possible values with those observed in the computations. We examine the implications of the more strict observed constraints. Throughout the thesis, we continuously demonstrate the deep connections between our object of study and the Four color theorem.

Chapter 1

Preliminaries

In this chapter, we will introduce the basic terminology and definitions used throughout this work. We will also present the widely known results that are crucial for our research and provide a motivational example to justify the usefulness of the introduced concepts.

1.1 Graphs and multipoles

Unless stated otherwise, graphs may contain loops and parallel edges. Graphs that can contain dangling edges are called multipoles—we will formalize such edges using special degree-one vertices. Let $H = (V, E)$ be a graph and T be an ordered k-tuple of distinct degree-one vertices in H. Then the pair $G = (H, T)$ is called a *k-pole*. Vertices in T are called *outer vertices*, and the remaining vertices are called *inner vertices. Outer edge* is an edge incident to an outer vertex and *inner edge* is an edge incident to two inner vertices. Note that under this definition, the common notion of a graph without dangling edges corresponds to a 0-pole $(H, \emptyset)$. Many terms and operations that are defined for the underlying graph H can be naturally introduced for the k-pole $G = (H, T)$. For instance, the symbol $G - e$ denotes the k-pole obtained by removing an inner edge e from G. Similarly, G/e denotes the k-pole obtained by contracting an inner edge e (that is not a loop) in G.

If $G = (H, T)$ has a planar embedding such that all vertices in T are on the outer face and their order on the face matches their order in T, then we call the embedding a *planar k-pole*. If every inner vertex in a k-pole G has degree 3, then G is called a *cubic k-pole*. The importance of cubic planar k-poles will become evident in the following sections when discussing the Four color theorem.

1.2 Colorings

Under the term m-coloring of a planar graph, we understand an assignment of at most m distinct colors to the vertices of the graph such that no two adjacent vertices have the same assigned color. An m-edge-coloring and an m-face-coloring are defined analogously.

One of the most fundamental results in graph theory is the following [1, ch. 5]:

Theorem 1.1 (Four color theorem)**.** *Every bridgeless planar graph admits a 4-face-coloring.*

If we consider the dual graph of a planar graph, we can see that the Four color theorem is equivalent to the statement that every planar graph without loops admits a 4-coloring of its vertices.

For any planar graph without loops, adding more edges while preserving planarity makes the vertex colorability of the graph even more difficult. If a graph has a face with four or more edges, we can add a diagonal to the face. That implies that if a counterexample to the dual formulation of the Four color theorem (where we are coloring vertices) existed, we could construct a counterexample that is also a triangulation. The dual graph to such a counterexample would be a bridgeless cubic planar graph, implying that proving Theorem 1.1 for bridgeless cubic planar graphs is sufficient to prove the entire theorem.

It can be shown [1, ch. 6.5] that the existence of a 4-face-coloring of a cubic planar graph is equivalent to the existence of its 3-edge-coloring. The idea is that if we assign an orientation to each edge and an element of a 4-element abelian group to each face color, each edge can be assigned the difference of the two group elements of the faces it separates (and vice versa; the edge orientation serves to determine which face should be subtracted from which). Since the adjacent faces have different colors, all edges obtain a non-zero value, forming a 3-edge-coloring. Favorably, we can use the 4-element group $(\mathbb{Z}_2 \times \mathbb{Z}_2, +)$ which has the property that every element is its own inverse. This renders the orientation of edges irrelevant, as reversing an edge orientation is equivalent to replacing the assigned group element with its inverse.

All in all, this means that the Four color theorem is equivalent to the statement that every bridgeless cubic planar graph admits a 3-edge-coloring. Bridgeless cubic graphs that are not 3-edge-colorable are called *snarks*, so a Four color theorem counterexample would be a planar snark.

We can view a part of a larger graph as a k-pole, so the 3-edge-colorability of cubic planar k-poles is closely tied to the 3-edge-colorability of cubic planar graphs.

An example of these ideas is shown in Figure 1.1. In the following section, we will introduce the concept of $(\mathbb{Z}_2 \times \mathbb{Z}_2)$-flows, which can be considered a generalization of 3-edge-colorings to non-cubic k-poles that we will use throughout this work.

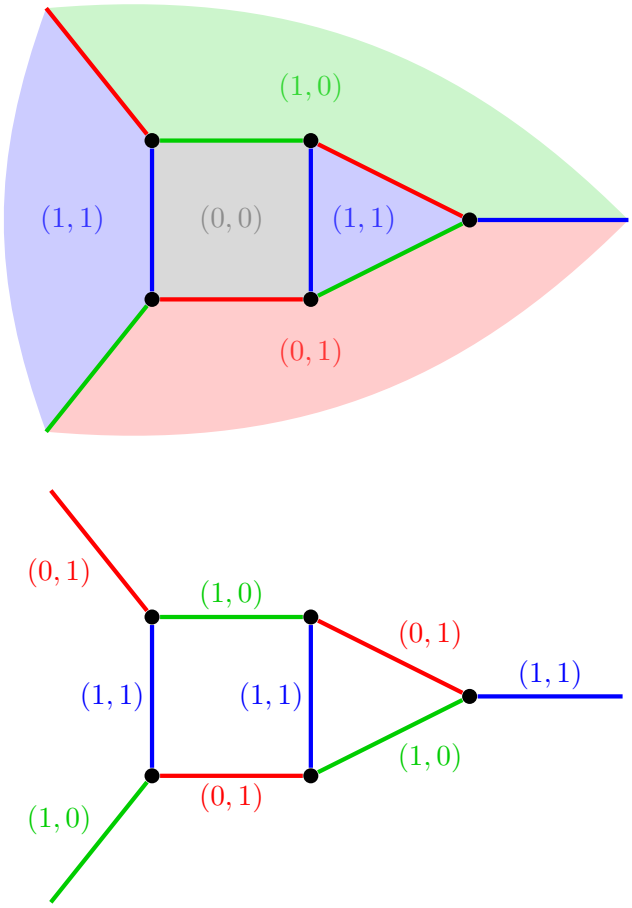

Figure 1.1: A 3-edge-coloring corresponding to a 4-face-coloring of a cubic planar 3-pole. Each edge color is obtained as a difference of the two adjacent face colors. Since we structure the colors as the group $(\mathbb{Z}_2 \times \mathbb{Z}_2, +)$ where every element is an involution, the order in which we subtract the face colors is irrelevant.

1.3 Flows

In general, the term *flow network* often refers to a directed graph with edge capacities and an assignment of non-negative real values to the edges that do not exceed the capacities. In contrast to this, we will focus on a slightly different concept. Instead of real values, we consider values from a finite abelian group assigned to the edges. Since assigning the value 0 to an edge effectively ignores it, only the non-zero values are allowed.

Let $\mathcal{G}$ be a finite abelian group. An assignment of orientations and *non-zero* values from $\mathcal{G}$ to the edges of $G = (H, T)$ is called a *$\mathcal{G}$-chain* in G. For a $\mathcal{G}$-chain ϕ in G, the difference between the sum of values on the edges entering a vertex v and the sum of values on the edges leaving v is called the *boundary of vertex v*.

A $\mathcal{G}$-chain ϕ is called a *$\mathcal{G}$-flow* if every vertex in G that is not in T has a boundary of 0. The *boundary of the $\mathcal{G}$-flow ϕ* is a k-tuple whose i-th element is equal to the

boundary of the i-th vertex in T for all $i \in \{1, \ldots, k\}$. This concept is often referred to as a *nowhere-zero flow*, but for simplicity, we will use only the term *flow*.

As we hinted in the previous section, 3-edge-colorings coincide with $(\mathbb{Z}_2 \times \mathbb{Z}_2)$-flows in cubic graphs, because three $\mathbb{Z}_2 \times \mathbb{Z}_2$ group elements sum to zero if and only if they are precisely the elements $(0,1), (1,0), (1,1)$. Throughout this work, we will therefore focus on $(\mathbb{Z}_2 \times \mathbb{Z}_2)$-flows in cubic k-poles, which also allows us to ignore the edge orientation. Nevertheless, we will point out which parts of our work are also meaningful for other groups and k-pole classes.

Lemma 1.1 (k-pole boundary sum)**.** *Let $\mathcal{G}$ be a finite abelian group, G be a k-pole, and ϕ be a $\mathcal{G}$-flow in G. Then the sum of the k-pole boundary is zero.*

Proof. This follows from the fact that the sum s of all inner vertex boundaries is, by definition, zero. Each inner edge is added to as well as subtracted from s, so it contributes zero to the sum. Each outer edge is accounted for only once in s. Let t be the k-pole boundary sum. This gives us $t = -s = 0$. □

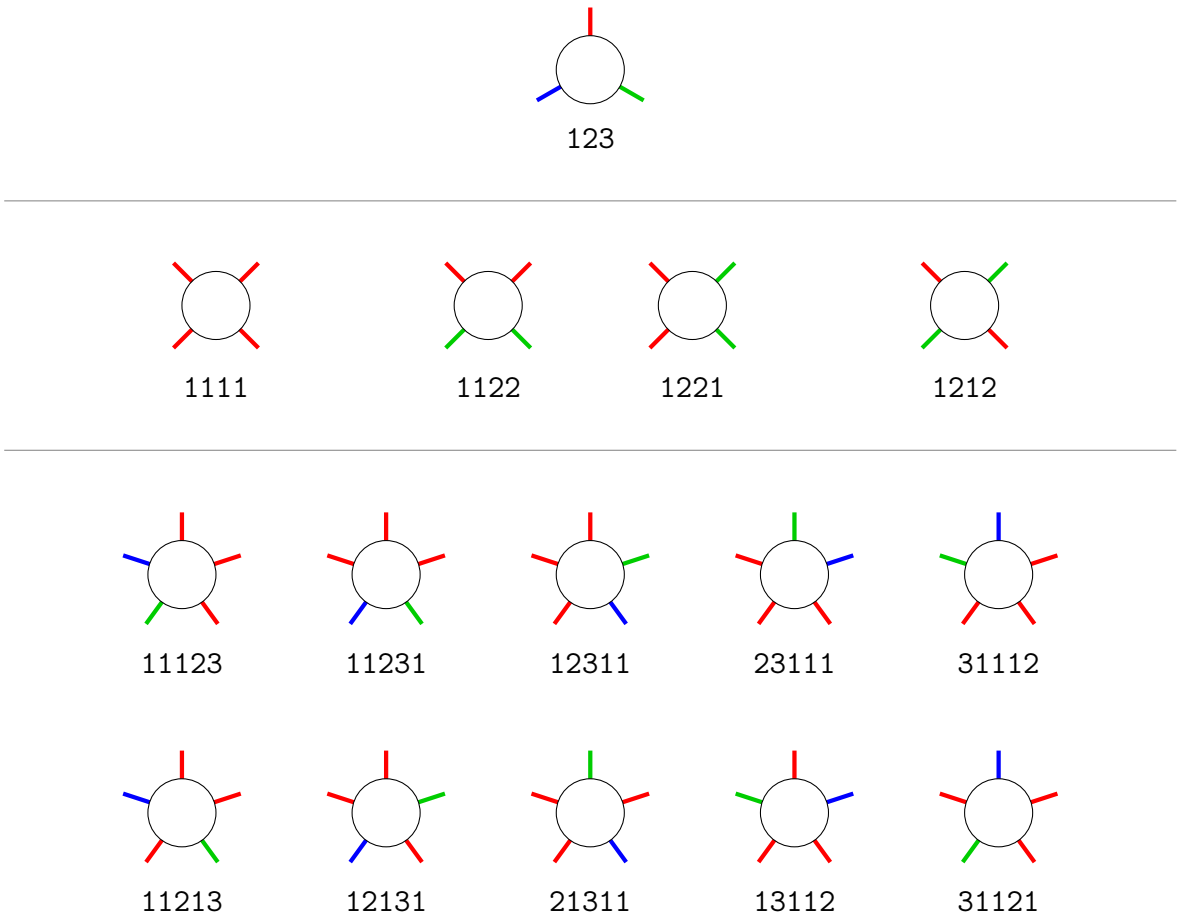

Figure 1.2: All admisssible boundaries of 3-, 4-, and 5-poles. The color permutations are not considered.

For instance, Lemma 1.1 implies that:

- no 1-pole has a $(\mathbb{Z}_2 \times \mathbb{Z}_2)$-flow (this also holds for any abelian group $\mathcal{G}$),
- every $(\mathbb{Z}_2 \times \mathbb{Z}_2)$-flow in a 2-pole assigns the same value to the two outer edges,
- every $(\mathbb{Z}_2 \times \mathbb{Z}_2)$-flow in a 3-pole assigns exactly the three different non-zero values to the three outer edges.

We will call k-tuples of non-zero elements from $\mathcal{G}$ that sum to zero *admissible boundaries*—these are the k-tuples that satisfy Lemma 1.1. All admissible boundaries for $k \in \{3, 4, 5\}$ are depicted in Figure 1.2. For simplicity, we will refer to the three edge colors (or the non-zero elements of $\mathbb{Z}_2 \times \mathbb{Z}_2$, respectively) as `1`, `2`, and `3`. As the color permutation is arbitrary, we will usually refer to the class of boundaries equivalent under color permutation. We will denote the number of admissible boundaries for a k-pole as $\sigma(k)$ and the i-th such boundary as $\beta_i^{(k)}$.

1.4 Multipole polynomial

Studying the edge 3-colorability of cubic planar k-poles is effectively equivalent to studying the number of $(\mathbb{Z}_2 \times \mathbb{Z}_2)$-flows in cubic planar k-poles. Let $f_\beta(G)$ denote the number of $\mathcal{G}$-flows in a given k-pole G with a given boundary β.

A loop in a G can be assigned any non-zero value. A non-loop edge can be contracted in G; the resulting k-pole has exactly the same flows as G—the value of the contracted edge is simply the difference of the two incident vertex boundaries (when undoing the contraction). There is an exception though—the flows where this difference is zero. Luckily, these are exactly the flows in a k-pole obtained from G by removing the edge. This gives us the following well-known formula [1, ch. 6.3]:

Theorem 1.2 (flow polynomial formula)**.** *Let G be a k-pole, β its boundary, and e its inner edge. Then the number of flows $f_\beta(G)$ over an abelian group $\mathcal{G}$ of order m satisfies the following:*

- $f_\beta(G) = (m-1) \cdot f_\beta(G-e)$ *if e is a loop,*
- $f_\beta(G) = f_\beta(G/e) - f_\beta(G-e)$ *otherwise.*

This formula naturally translates to a recursive algorithm—each step computes the numbers of flows in smaller k-poles and combines them accordingly. The base cases of the recursion are the numbers of flows in k-poles with no inner edges, where outer edges are gathered in groups of edges incident to a common inner vertex.

Definition 1.1 (basic k-pole)**.** A k-pole G is called *basic* if it has no inner edges.

The number of flows is traditionally computed for graphs (i.e. 0-poles), where the base case is a graph with no edges, which has trivially a single empty flow. If we consider the value m a parameter, the resulting expression given by the recursion in Theorem 1.2 is a polynomial in m. This polynomial is commonly known as the *flow polynomial*. It can also be extended to a general concept called *Tutte polynomial* [2, 3].

However, if we fix m to a specific value (4 in our case) and consider the basic k-poles as symbols, the recursive computation results in $f_\beta(G)$ being expressed as a linear combination of the symbols (since this holds for both the base case and the recursive step).[1]

Given that each step of the recursion operates on a single edge, it should be obvious that the coefficients of the linear combination are unique irrespective of the order in which the edges are processed. The boundary β then determines the numbers of flows in the basic k-poles—each one is either 0 or 1, depending on whether β is *compatible* with the basic k-pole according to Lemma 1.1 for each group of adjacent outer edges.

The recursive formula gives the same linear combination of symbols for any admissible boundary β. Selecting a specific boundary thus means transforming the linear combination of basic k-poles into a single numeric constant (the number of flows with the given boundary).

Let us call k-poles with no degree-one inner vertices *proper* k-poles. Since a non-proper basic k-pole is not compatible with any boundary, its coefficient is irrelevant. We can, therefore, restrict our attention to proper basic k-poles only. Furthermore, the recursion preserves planarity. Even though these observations hold in general, we will focus on the planar case. The proper planar basic k-poles for small values of k are shown in Figure 1.3. Since in the group $\mathbb{Z}_2 \times \mathbb{Z}_2$, a degree-two vertex can be smoothed out (the two incident edges must be assigned the same value in every flow), we will consider only basic k-poles with no degree-two inner vertices to eliminate representing the same basic k-pole in several different ways.

We will denote the number of proper planar basic k-poles as $\pi(k)$ and the i-th such k-pole as $P_i^{(k)}$. For small values of k, we introduced unique names for the basic k-poles, as shown in Figure 1.3.

[1] At this point, it should be clear why introducing flows instead of discussing plain edge colorings is useful: the recursive formula does not hold for edge colorings. Since we are interested in the coefficients of basic k-poles, flows serve as a good generalization of edge colorings, because they behave well under the recursive formula, down to the base case.

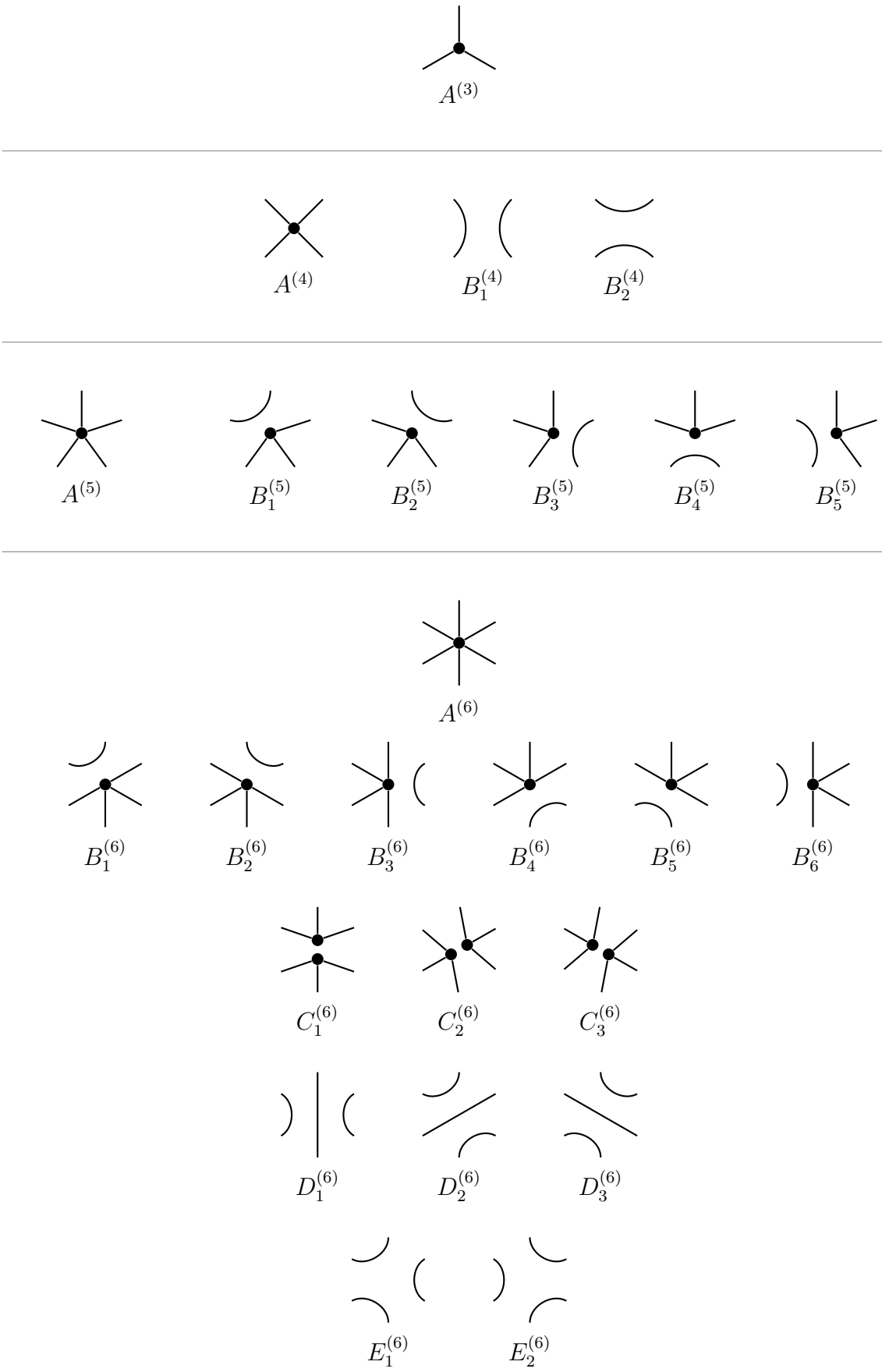

Figure 1.3: All proper planar basic 3-, 4-, 5-, and 6-poles.

Let us now condense the above observations in a more formal way.

Definition 1.2 (multipole polynomial)**.** Let G be a planar k-pole. If we recursively apply Theorem 1.2 until we reach the basic k-poles and combine the results, we obtain a linear combination of the proper planar basic k-poles $P_i^{(k)}$ for $i \in \{1, \ldots, \pi(k)\}$ with integer coefficients. We will call this expression the *multipole polynomial* of G and the tuple of coefficients the *multipole polynomial coefficients* of G.

Theorem 1.3. *Let G be a planar k-pole and $(c_1, \ldots, c_{\pi(k)})$ be its multipole polynomial coefficients. Then for every admissible boundary β, the number of flows $f_\beta(G)$ over the group $(\mathbb{Z}_2 \times \mathbb{Z}_2, +)$ is equal to*

$$\sum_{i=1}^{\pi(k)} c_i \cdot f_\beta(P_i^{(k)})$$

where $f_\beta(P_i^{(k)})$ is either 0 or 1 depending on whether β is compatible with the basic k-pole $P_i^{(k)}$.

Example 1.1. An illustration of this concept for $\beta = \texttt{1221}$ is shown in Figure 1.4. The multipole polynomial coefficients of the example 4-pole are $(0, 1, 1)$.

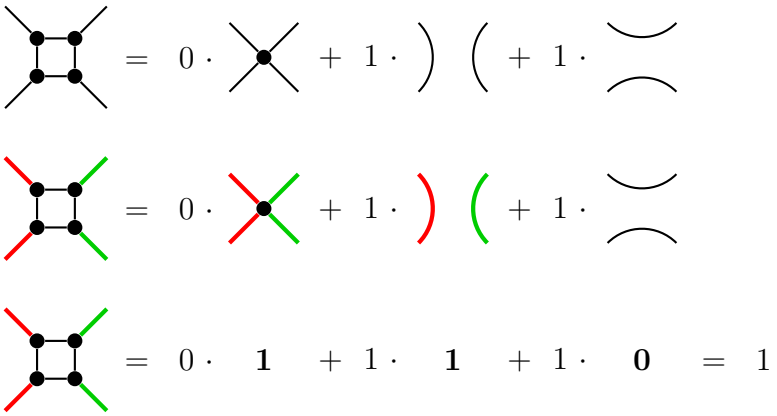

Figure 1.4: An illustration of the multipole polynomial.

According to our knowledge, the idea of the multipole polynomial was first described and utilized by Kochol [4] and subsequently used in several more papers [5, 6, 7] or touched upon indirectly [8, lem. 4.2]. Similar methods were also applied in a slightly different context during the study of chromatic polynomials [9, 10].

Kochol used the multipole polynomial with the group $(\mathbb{Z}_5, +)$ to determine some properties of a counterexample to the 5-flow conjecture—another famous problem in graph theory. In our work, we will study the power of the multipole polynomial coefficients in relation to the Four color theorem.

1.5 Motivation

Let us illustrate the usefulness of the multipole polynomial. Consider the following example. Let G be a cubic planar 4-pole which has:

$$\text{an unknown number of } \texttt{1111} \text{ colorings:} \quad 0 \leq f_{\texttt{1111}}(G) \tag{1.1}$$

$$\text{no } \texttt{1221} \text{ colorings:} \quad 0 = f_{\texttt{1221}}(G) \tag{1.2}$$

$$\text{no } \texttt{1122} \text{ colorings:} \quad 0 = f_{\texttt{1122}}(G) \tag{1.3}$$

$$\text{a non-zero number of } \texttt{1212} \text{ colorings:} \quad 0 < f_{\texttt{1212}}(G) \tag{1.4}$$

As we observed in the previous chapter, there exist constants a, b_1, b_2 such that the following equation holds for every boundary β of G:

$$f_\beta(G) = a \cdot f_\beta(A^{(4)}) + b_1 \cdot f_\beta(B_1^{(4)}) + b_2 \cdot f_\beta(B_2^{(4)})$$

For each boundary β, we can evaluate f_β for each of the basic 4-poles like in Example 1.1—its value is either 0 or 1, depending on whether the boundary is compatible with the basic 4-pole. Combined with eqs. (1.1) to (1.4), this gives us the following system of constraints on the constants a, b_1, b_2:

$$\beta = \texttt{1111}: \quad 0 \leq a + b_1 + b_2 \tag{1.5}$$

$$\beta = \texttt{1221}: \quad 0 = a + b_1 \tag{1.6}$$

$$\beta = \texttt{1122}: \quad 0 = a + b_2 \tag{1.7}$$

$$\beta = \texttt{1212}: \quad 0 < a \tag{1.8}$$

From eqs. (1.6) and (1.7) we have $b_1 = b_2 = -a$, which gives $a + b_1 + b_2 = a - a - a = -a < 0$, from eq. (1.8). However, this contradicts eq. (1.5). As a result, the system of constraints is inconsistent, which means that no 4-pole with properties (1.1) to (1.4) exists.

The same conclusion can be reached by a different argument, which uses the concept of Kempe chains. Let G be a 3-edge-colored cubic planar 4-pole with outer vertices u and v. A `1-2` *Kempe chain* between u and v is a path that starts at u, ends at v, and alternates between colors `1` and `2`.

Let v_1, v_2, v_3, v_4 be the outer vertices of a cubic planar 4-pole G that satisfies eqs. (1.1) to (1.4). Suppose that it is colored by one of the `1212` colorings. If we start at v_1 and follow edges of color `1` and `2` alternately, we will eventually reach another outer vertex, since each inner vertex has exactly one edge of each color, so we can always continue the path until we reach a different outer vertex. The resulting path is a `1-2` Kempe chain p.

Suppose that the ending vertex of p is v_2. In that case, we can flip the colors of p and obtain a valid `2112` coloring (that is, a coloring of type `1221`), which contradicts

eq. (1.2). Similarly, if the ending vertex of p is v_4, we can flip the colors of p and obtain a valid `2211` coloring (that is, a coloring of type `1122`), which contradicts eq. (1.3). Therefore, p has to end at v_3. Equivalently, if we construct a `1-2` Kempe chain q starting at v_2, we arrive at the conclusion that q has to end at v_4.

Given the order of vertices v_1, v_2, v_3, v_4 in the outer face of G, paths p and q must intersect. As G is planar, no two edges can cross each other, so p and q must share a vertex. However, this contradicts a simple observation that apart from the edges in p, the vertices of p are incident only with edges of color `3`, so no edge in q can be incident with a vertex in p, and therefore p and q cannot share a vertex. This contradiction shows that no cubic planar 4-pole with properties (1.1) to (1.4) exists.

The multipole polynomial method results in the same outcome but does not require the use of such a powerful structural concept as Kempe chains. This demonstrates that the multipole polynomial coefficients carry significant information about the structure of a k-pole.

Chapter 2

Coefficient counts

In the previous chapter, we examined four constraints on the flow counts for the four admissible boundaries (not taking color permutation into account) of a cubic planar 4-pole. These four expressions utilized only three variables—the coefficients a, b_1, b_2. A natural question arises: Can the numbers of flows for all admissible boundaries of a k-pole be condensed into a smaller number of coefficients for all possible values of k? Let us answer this question in this chapter by inspecting the values of the two quantities.

The admissible boundaries of a k-pole can be matched to 4-edge-colorings of a k-cycle: We can construct an admissible boundary by choosing elements equal to the difference of the adjacent edge colors in any given 4-edge-coloring of a k-cycle, and vice-versa. If we consider the classes of admissible boundaries and 4-edge-colorings up to color permutation, we can see that this mapping is bijective. The number $\sigma(k)$ of the admissible boundaries is thus equal to the number of 4-edge-colorings of a k-cycle, which corresponds to the OEIS sequence A006342 [11]. It can be shown [12] that

$$\sigma(k) = \begin{cases} \frac{3^{k-1}+5}{8} & \text{if } k \text{ is even,} \\ \frac{3^{k-1}-1}{8} & \text{if } k \text{ is odd.} \end{cases}$$

Asymptotically, $\sigma(k) \sim \frac{3^k}{24}$.

On the other hand, proper planar basic k-poles correspond to non-crossing partitions of k that contain no singletons. Their counts $\pi(k)$, also known as *Riordan numbers*, were studied in several different contexts and are assigned the OEIS sequence A005043 [13]. Even though the sequence has no explicit formula, it can be described [14] by the recurrent relation

$$\pi(k+1) = \frac{k}{k+2}\left(2\pi(k) + 3\pi(k-1)\right).$$

The sequence's asymptotical behavior [13] is $\pi(k) \sim \frac{3^k}{k^{3/2}\frac{8}{9}\sqrt{3\pi}}$. This shows that $\pi(k)$ is asymptotically smaller than $\sigma(k)$. It is also smaller even for small values of k, as shown in Table 2.1.

k	$\sigma(k)$	$\pi(k)$
2	1	1
3	1	1
4	4	3
5	10	6
6	31	15
7	91	36
8	274	91
9	820	232
10	2461	603
11	7381	1585
12	22144	4213
13	66430	11298
14	199291	30537

Table 2.1: Comparison of the number $\sigma(k)$ of admissible boundaries of k-poles and the number $\pi(k)$ of proper planar basic k-poles for small values of k [11, 13].

It is not difficult to prove the strict inequality between the two quantities:

Theorem 2.1. *For all $k \geq 4$, the number of admissible boundaries of a k-pole is strictly greater than the number of proper planar basic k-poles, $\sigma(k) > \pi(k)$.*

Proof. Given the formula for $\sigma(k)$, we see that $\sigma(k) \geq \frac{3^k}{24} - \frac{1}{8}$.

For $\pi(k)$, we will prove the following pair of inequalities for $k \geq 3$ by induction:

$$3\frac{k}{k+2}\pi(k) \leq \pi(k+1) \leq 3\pi(k)$$

This holds for the base case $k = 3$, as $\frac{9}{5} \leq 3 \leq 3$. Let us prove the induction step for $k \geq 4$, while assuming the inequalities for $k - 1$:

$$3\frac{k-1}{k+1}\pi(k-1) \leq \pi(k) \leq 3\pi(k-1)$$

Using the recurrent relation for $\pi(k)$, the induction hypothesis can be written as:

$$\begin{array}{rcccl} 3\frac{k}{k+2}\pi(k) & \leq & \frac{k}{k+2}\big(2\pi(k) + 3\pi(k-1)\big) & \leq & 3\pi(k) \\ 3k\pi(k) & \leq & 2k\pi(k) + 3k\pi(k-1) & \leq & (3k+6)\pi(k) \\ \pi(k) & \leq & 3\pi(k-1) & \leq & \frac{k+6}{k}\pi(k) \end{array}$$

The left inequality is satisfied by the induction assumption. The induction assumption also gives us $3\pi(k-1) \leq \frac{k+1}{k-1}\pi(k)$, so showing that $\frac{k+1}{k-1}\pi(k) \leq \frac{k+6}{k}\pi(k)$ is sufficient to

prove the induction step. This is equivalent to $k(k+1) \leq (k+6)(k-1)$ and simplifies to $6 \leq 4k$, which is of course true for all $k \geq 4$.

This grants $\pi(k+1) \leq 3\pi(k)$ for all $k \geq 3$. When applied i times consecutively, this translates to $\pi(k+i) \leq 3^i\pi(k)$ for all $i \geq 1$. Specifically, $\pi(k) \leq 3^{k-3}\pi(3) = \frac{3^k}{27}$ for $k \geq 4$. Putting together with the inequality for $\sigma(k)$, we get:

$$\pi(k) \leq \frac{3^k}{27} < \frac{3^k}{24} - \frac{1}{8} \leq \sigma(k)$$

The central inequality is equivalent to $27 < 3^k$, which holds for all $k \geq 4$. □

The presented result can be rephrased as follows: If we think of the vector $(f_{\beta_1^{(k)}}(G), \ldots, f_{\beta_{\sigma(k)}^{(k)}}(G))$ as coordinates of a planar k-pole G in a $\sigma(k)$-dimensional space, the subspace of all planar k-poles is actually of lower dimension $\pi(k)$, since each value $f_\beta(G) = \sum_{i=1}^{\pi(k)} c_i f_\beta(P_i^{(k)})$ is entirely determined by a subset of the $\pi(k)$ coefficients c_i.

However, it is important to note that this is only true for planar k-poles. The number of all (not necessarily planar) proper basic k-poles grows superexponentially [15], so the coefficients are not an efficient way to represent the flow counts for given boundaries in general. The property is, therefore, an interesting feature arising from planarity.

Since the flow counts for the admissible boundaries are determined by a smaller number of coefficients, we could ask whether the transformation is reversible, i.e. whether the coefficients can be unambiguously reconstructed from the flow counts. Let us assemble a matrix $M^{(k)}$ with $\sigma(k)$ rows and $\pi(k)$ columns, where the element $M_{i,j}^{(k)}$ is either 0 or 1, depending on whether the boundary $\beta_i^{(k)}$ is compatible with the basic k-pole $P_j^{(k)}$. Our question can then be equivalently stated as whether the matrix $M^{(k)}$ has the full rank, $\pi(k)$. We did not manage to prove this property for all values of k, but we verified it for $k \leq 13$ by directly evaluating the matrix rank. The SageMath code used for the verification is available in Appendix A. For $k = 14$, the matrix has $\sigma(14) \cdot \pi(14) > 6 \cdot 10^9$ elements, hitting the memory limit of a personal computer.

Chapter 3

Multipole connectivity

In this chapter, we will investigate the relationship between the multipole polynomial coefficient values and the connectivity properties of a cubic planar multipole.

Let p, r be non-negative integers and let $G = (H, T)$ be a planar $(p + r)$-pole such that $T = (u_1, u_2, \ldots, u_p, v_1, v_2, \ldots, v_r)$. If there exists a path in G connecting a vertex from $\{u_1, \ldots, u_p\}$ to a vertex from $\{v_1, \ldots, v_r\}$, we say that the multipole G is (p, r)-*connected*. Otherwise, it is (p, r)-*disconnected*.

Suppose that G is a (p, r)-connected $(p + r)$-pole. Let U, V be a partition of the vertices such that $\{u_1, \ldots, u_p\} \subseteq U$ and $\{v_1, \ldots, v_r\} \subseteq V$. Let C be the set of edges that have one endpoint in U and the other in V. Clearly, there is no path from U to V in $G - C$. If the set C contains only inner edges, it is called a (p, r)-*c-cut* of G where $c = |C|$. A (p, r)-1-cut C is called a (p, r)-*bridge*. A $(p + r)$-pole is (p, r)-*2-connected* if it is (p, r)-connected and has no (p, r)-bridge.

Note that a $(0, k)$-disconnected k-pole G is not interesting: It consists of a 0-pole Z disconnected from the rest of the k-pole, G'. The flows in Z and G' are independent. Let c_Z be the number of flows in Z and $(c'_1, \ldots, c'_{\pi(k)})$ be the multipole polynomial coefficients of G'. Thanks to independence, the coefficients of G must be $(c_Z \cdot c'_1, \ldots, c_Z \cdot c'_{\pi(k)})$. The component Z thus poses only as a multiplicative factor to the coefficients of G'.

If a k-pole G contains a $(0, k)$-bridge e, then e separates two parts of G: let Z be the one with no outer edges. If we consider e an outer edge of Z, then Z forms a 1-pole, which does not contain a flow (by Lemma 1.1). In other words, if we process all inner edges in Z according to Theorem 1.2, then focus our attention on any single of the resulting computation branches, and finally process the edge e in the remaining G', the result of $f_\beta(G'/e) - f_\beta(G' - e)$ will be a zero polynomial (because G'/e and $G' - e$ are equivalent with respect to the rest of the computation). Therefore, the coefficients of G must all be zeros. We will call such a bridge (i.e. an inner edge separating a part of the k-pole with no outer vertices) a *trivial bridge*.

Similarly to the $(0,k)$-disconnected k-poles, a k-pole G with a $(1,k-1)$-bridge is not interesting: The bridge separates a 2-pole Z from a smaller k-pole G'. Lemma 1.1 grants that any flow in G assigns the same value to the two outer edges in Z. The flows in Z and G' are independent (apart from the choice of the bridge value). Again, the number of flows in Z (for a fixed bridge value) poses only as a multiplicative factor to the coefficients of G'.

Finally, let $e_1, \ldots, e_p, h_1, \ldots, h_r$ be the outer edges incident with the outer vertices $u_1, \ldots, u_p, v_1, \ldots, v_r$. We will call a boundary (p,r)-*balanced* if the values assigned to $e_1, \ldots, e_p$ sum to zero (thanks to Lemma 1.1, this is equivalent to the values assigned to $h_1, \ldots, h_r$ summing to zero). Otherwise, the boundary is (p,r)-*unbalanced*. A flow is (p,r)-balanced if its boundary is (p,r)-balanced.

We are now equipped to formulate the main results of this chapter.

3.1 (p,r)-connectedness indicator

Theorem 3.1. *Let p, r be positive integers and G be a cubic planar $(p+r)$-pole without a trivial bridge. Then G is (p,r)-connected if and only if the sum I of flow counts $f_\beta(G)$ over all (p,r)-unbalanced admissible boundaries β is non-zero.*

Proof. Assume that $p, r \geq 2$. We will prove both implications by contradiction. Suppose that G is (p,r)-connected and $I = 0$. Let $e_1, \ldots, e_p, h_1, \ldots, h_r$ be the outer edges incident with the outer vertices $u_1, \ldots, u_p, v_1, \ldots, v_r$. Let us add two vertices u, v to G and the following edges, together forming a cubic planar graph H':

$$\begin{aligned} &\{(u_1,u_2),(u_2,u_3),\ldots,(u_{p-1},u_p)\} \\ \cup\ &\{(v_1,v_2),(v_2,v_3),\ldots,(v_{r-1},v_r)\} \\ \cup\ &\{(u_1,u),(u_p,u),(v_1,v),(v_r,v),(u,v)\} \end{aligned}$$

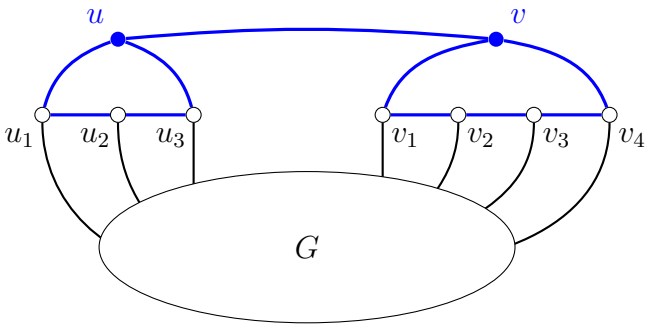

Figure 3.1: An illustration of the $(3,4)$-connectedness extension. The original 7-pole is labeled G; the vertices and the edges of the extension are in blue.

The multipole extension is illustrated in Figure 3.1. Assume that there exists a flow ϕ in the extended planar graph H' and let s and t be the sums of values assigned

to the edges $e_1, \ldots, e_p$ and $h_1, \ldots, h_r$, respectively. Since $I = 0$, the flow ϕ must be (p,r)-balanced in the original G, i.e. $s = t = 0$. If x is the flow value assigned to the edge (u,v), we can restrict our focus to the $(p+1)$-pole formed by the cycle $u_1, \ldots, u_p, u$ with the outer edges $e_1, \ldots, e_p, (u,v)$. Lemma 1.1 then implies that $s + x = 0$ (and similarly, $t + x = 0$). Combined with $s = 0$, we get $x = 0$, which is a contradiction with the definition of a flow. In other words, the extension admits only (p,r)-unbalanced flows, whereas G admits only (p,r)-balanced flows.

This means that no flow ϕ exists in H'. We know that G contains no trivial bridge. Any other bridge in G must be in a path connecting two outer vertices. If the two vertices are u_i, v_j, then they are connected also by the path $u_i, \ldots, u_p, u, v, v_1, \ldots, v_j$ in the extension, thus the bridge is no longer a bridge in H'. Similarly, if the two outer vertices are u_i, u_j (or v_i, v_j, respectively), they are connected also by the path $u_i, \ldots, u_j$ in the extension. Therefore, H' is a bridgeless cubic planar graph with no flows, which contradicts the Four color theorem.

On the other hand, suppose that G is (p,r)-disconnected and $I > 0$. Then G can be regarded as the union of a separated p-pole G_1 and r-pole G_2. Lemma 1.1 then tells us that the G_1 boundary must sum to zero, and the G_2 boundary must sum to zero as well. Every flow in G is thus (p,r)-balanced, which contradicts $I > 0$.

Finally, let us deal with the small cases. If $p = 1$, we can identify u with u_1 in the extension and the rest of the argumentation holds as before. The $r = 1$ case is equivalent. □

Theorem 3.1 is interesting in our context because each value $f_\beta(G)$ is a sum of a subset of multipole polynomial coefficients (the ones that correspond to the basic k-poles compatible with β), as stated in Theorem 1.3 and illustrated in Section 1.5. For the given values p, r, the indicator I is thus a fixed linear combination of the multipole polynomial coefficients.

Example 3.1. Let us provide an example for $p = r = 2$. As shown in Section 1.5, the numbers of flows with the boundaries `1111`, `1221`, `1122`, and `1212` in a cubic planar 4-pole G with the multipole polynomial coefficients a, b_1, b_2 are as follows:

$$f_{1111}(G) = a + b_1 + b_2$$
$$f_{1221}(G) = a + b_1$$
$$f_{1122}(G) = a + b_2$$
$$f_{1212}(G) = a$$

Only the boundaries `1221` and `1212` are $(2,2)$-unbalanced. The indicator value can therefore be expressed as $I = f_{1221}(G) + f_{1212}(G) = 2a + b_1$. The result is that G is $(2,2)$-connected if and only if $2a + b_1 > 0$.

Corollary 3.2. *The Four color theorem is equivalent to the non-existence of a* $(2,2)$*-connected cubic planar 4-pole without a trivial bridge that has* $2a + b_1 = 0$.

Proof. If the Four color theorem holds, then the other statement is true by Theorem 3.1.

If we had a planar snark (a counterexample to the Four color theorem), we could select any edge (u, v), remove it together with the vertices u and v, and consider the adjacent edges the outer edges of the remaining 4-pole. Since (u, v) could not be a bridge in the snark, the resulting 4-pole must be $(2, 2)$-connected. The value of $2a + b_1$ would have to be zero, because otherwise, the 4-pole would have a $(2, 2)$-unbalanced flow, which contradicts the uncolorability of the snark. □

Our proof of Theorem 3.1 relies on the Four color theorem. However, Corollary 3.2 shows that managing to prove Theorem 3.1 without relying on the Four color theorem would result in an alternative proof of the Four color theorem.

Theorem 3.1 can also be refined into another, perhaps even more interesting statement:

Theorem 3.3. *Let* p, r *be positive integers and* G *be a cubic planar* $(p+r)$*-pole without a trivial bridge. Then* G *is* (p, r)*-connected if and only if at least one of its multipole polynomial coefficients corresponding to* (p, r)*-connected basic* $(p + r)$*-poles is non-zero.*

Proof. If G is (p, r)-connected, then according to Theorem 3.1, there must be at least one (p, r)-unbalanced boundary β that yields non-zero $f_\beta(G)$. Let B be the set of basic $(p+r)$-poles that are compatible with β. The value of $f_\beta(G)$ is a sum of the coefficients corresponding to the elements of B, so at least one of these coefficients must be non-zero. Furthermore, none of the basic $(p + r)$-poles in B can be (p, r)-disconnected, since it would only be compatible with (p, r)-balanced boundaries, as per Lemma 1.1. Therefore, it can be concluded that one of the coefficients corresponding to (p, r)-connected basic $(p + r)$-poles in B must be non-zero.

On the other hand, if G is (p, r)-disconnected, the recursive computation defined by Theorem 1.2 can never reach a (p, r)-connected basic $(p + r)$-pole, resulting in all the corresponding coefficients being zero. □

In the context of Example 3.1, the $(2, 2)$-connected basic 4-poles are $A^{(4)}$ and $B_1^{(4)}$ (note that in Figure 1.3, the outer edges e_1, e_2 correspond to the upper ones and the outer edges h_1, h_2 correspond to the lower ones). Theorem 3.3 then states that a cubic planar 4-pole G without trivial bridges is $(2, 2)$-connected if and only if one of the coefficients a, b_1 is non-zero.

Planarity is, however, necessary for these results to hold: Let us consider a Petersen graph where an edge is removed, and the four adjacent edges are considered the outer edges of a 4-pole, like in Figure 3.2. The coefficients of this 4-pole are $a = 0, b_1 = 0, b_2 = 2$

(note that there is also one non-planar basic 4-pole, but its coefficient is 0 in this case). This 4-pole is $(2, 2)$-connected, but the indicator $I = 2a + b_1$ is zero, so Theorem 3.1 does not hold (and neither does Theorem 3.3). This example shows that the indicator is indeed valid only for planar multipoles.

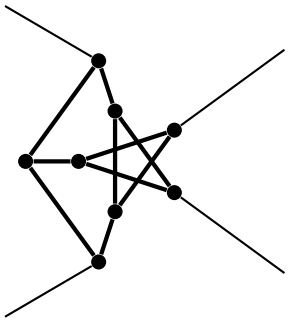

Figure 3.2: A non-planar counterexample to Theorem 3.1.

3.2 (p, r)-2-connectedness indicator

Theorem 3.4. *Let p, r be integers greater than one and G be a cubic planar (p, r)-connected $(p + r)$-pole without a trivial bridge. Then G is (p, r)-2-connected if and only if the sum J of flow counts $f_\beta(G)$ over all (p, r)-balanced admissible boundaries β is non-zero.*

Proof. Suppose that G is (p, r)-2-connected and $J = 0$. Let $e_1, \ldots, e_p, h_1, \ldots, h_r$ be the outer edges incident with the outer vertices $u_1, \ldots, u_p, v_1, \ldots, v_r$. Let us add the following edges to G, forming a cubic planar graph H':

$$\{(u_1, u_2), (u_2, u_3), \ldots, (u_{p-1}, u_p), (u_p, u_1)\}$$
$$\cup \{(v_1, v_2), (v_2, v_3), \ldots, (v_{r-1}, v_r), (v_r, v_1)\}$$

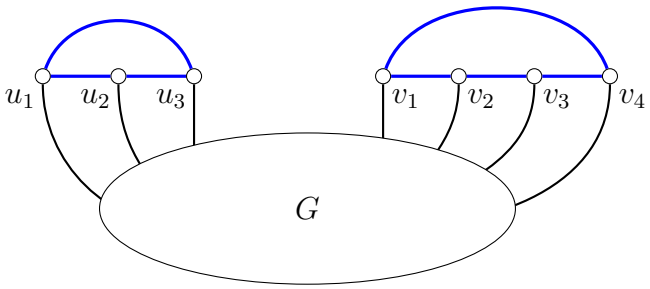

Figure 3.3: An illustration of the $(3, 4)$-2-connectedness extension. The original 7-pole is labeled G; the edges of the extension are in blue.

The extension corresponds to a p-cycle and an r-cycle, as illustrated in Figure 3.3. Assume that there exists a flow ϕ in the extended planar graph H' and let s and t be

the sums of values assigned to the edges $e_1, \ldots, e_p$ and $h_1, \ldots, h_r$, respectively. Since $J = 0$, the flow ϕ must be (p, r)-unbalanced in the original G, i.e. $s \neq 0$. If we consider the added p-cycle a p-pole with outer edges $e_1, \ldots, e_p$, Lemma 1.1 implies that $s = 0$, which is a contradiction (similar reasoning can be applied to t). In other words, the extension admits only (p, r)-balanced flows, whereas G admits only (p, r)-unbalanced flows.

This means that no flow ϕ exists in H'. We know that G contains no trivial bridge and no (p, r)-bridge. Any other bridge in G must be in a path connecting two outer vertices u_i, u_j (or symmetrically, v_i, v_j). Then they are connected in H' also by the path $u_i, \ldots, u_j$ in the extension. Therefore, H' is a bridgeless cubic planar graph with no flows, which contradicts the Four color theorem.

On the other hand, suppose that G is not (p, r)-2-connected and $J > 0$. Then G contains a (p, r)-bridge e, where e separates a $(p + 1)$-pole G_1 from an $(r + 1)$-pole G_2. Let ϕ be a (p, r)-balanced flow in G, x the value it assigns to e and s the sum of the values assigned to the edges $e_1, \ldots, e_p$. Lemma 1.1 for G_1 implies that $s + x = 0$, but since ϕ is (p, r)-balanced, $s = 0$, which results in $x = 0$, a contradiction. □

Like in the previous section, the indicator J can be expressed as a fixed linear combination of the multipole polynomial coefficients for given values p, r. Continuing the Example 3.1, the only $(2, 2)$-balanced boundaries are `1111` and `1122`. The indicator value is therefore $J = f_{1111}(G) + f_{1122}(G) = 2a + b_1 + 2b_2$, so a $(2, 2)$-connected cubic planar 4-pole G without trivial bridges is $(2, 2)$-2-connected if and only if $2a+b_1+2b_2 > 0$.

Unfortunately, an equivalent of Theorem 3.3 for (p, r)-2-connectedness cannot be formulated, since the fact that a boundary is (p, r)-balanced does not identify a property of basic $(p + r)$-poles, in contrast to the case of Theorem 3.3.

Chapter 4

Computation

As a part of this work, we will explore the computational aspect of determining the multipole polynomial coefficients. We will describe basic recursion with memoization, as well as a more advanced general approach that exploits the multipole structure to enable more efficient computation. We will also briefly compare the performance of both algorithms on cubic planar multipoles.

4.1 Naive algorithm

The simplest solution is computing the coefficients recursively, utilizing the recursive formula laid out in Theorem 1.2 directly. This would, unfortunately, result in an exponential number of recursive calls, which is infeasible even for a few tens of inner edges, regardless of the k-pole structure. As a remedy, we can utilize memoization to store the coefficients for smaller k-poles during the computation to reuse them later. This may be very efficient if the smaller k-poles that appear during the recursion are often repeated. On the other hand, if repetition is rare, we gain little from this approach and introduce an increased memory consumption.

4.2 Sequential algorithm

If we want to avoid the exponential branching of the naive algorithm, we can compute the coefficients in a sequential manner—one vertex at a time. The algorithm computes the coefficients of a k-pole G in several steps. In each step, the following procedure is performed:

1. A single inner vertex v is selected.
2. The vertex v is cut off from the rest of the k-pole by removing all its incident outer edges O_v and converting all its incident inner edges I_v to new outer edges. This way, a smaller k'-pole G' is created.

3. The multipole polynomial of G' is computed recursively.

4. The vertex v is attached to the basic k'-poles in the multipole polynomial of G', transforming them into small (possibly non-basic) k-poles.

5. The multipole polynomials of the small k-poles are computed by applying Theorem 1.2 to the edges I_v. Putting them together, we obtain the multipole polynomial of G.

An example of the sequential algorithm computation step is illustrated in Figure 4.1. The last step computes the final coefficients as $a = 2a' + b'_1$, $b_1 = 0$, and $b_2 = a' + 3b'_2$.

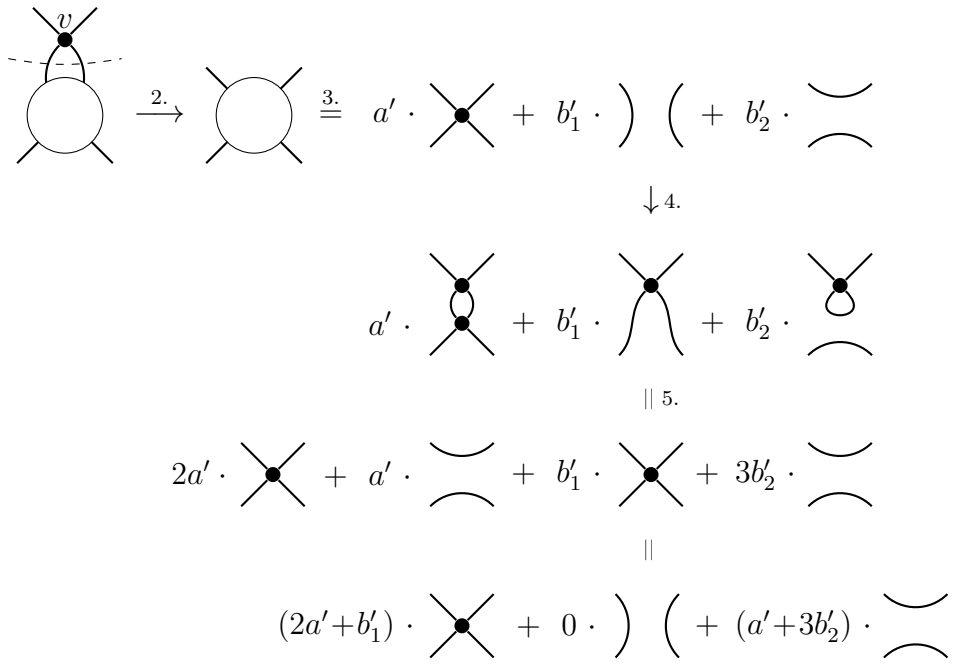

Figure 4.1: An illustration of the sequential algorithm computation step.

There are several aspects of the algorithm we need to comment on. Most importantly, the time complexity is not necessarily subexponential, despite the sequential nature of the algorithm. The reason is that if $|I_v| > |O_v|$, we obtain $k' > k$, and since the number of basic k-poles grows exponentially with k (see Chapter 2), the recursive call may return many different basic k'-poles (in general, exponential in the number of outer edges), and processing them may be the time complexity bottleneck.

However, this property is also the strength of the algorithm. We can utilize the value $|I_v| - |O_v|$ as a vertex selection heuristic. Selecting the vertex with the lowest $|I_v| - |O_v|$ value in each step, we can expect that k will grow slowly (or even decrease) during the computation, restricting the time complexity greatly. This is particularly true if we consider only cubic k-poles: If we assume that there is at least a single outer edge, cutting off its incident inner vertex will either decrease k by 1 (if the vertex is

incident with two outer edges) or increase k by 1 (if the vertex is incident with a single outer edge). It is reasonable to expect that we will typically encounter the former case often enough to observe a satisfactory performance.

We can view the sequential approach as an improved version of the naive algorithm, where we are contracting and deleting a batch of adjacent inner edges at each step, instead of a single edge. Note that the sequential algorithm principle is also applicable to other commutative groups, not only $\mathbb{Z}_2 \times \mathbb{Z}_2$.

In the rest of this section, we will describe some of the further improvements to the sequential algorithm.

Vertex selection heuristic refinement

We stated that we select the vertex that contributes the least outer edges when cut off, i.e. the vertex v with the lowest $|I_v| - |O_v|$ value. However, for general graphs that may contain parallel edges, this is not completely accurate. If $|O_v|$ outer edges are incident with v in a k-pole and $|O_v| > 0$, then the basic k-poles that we can reach during the computation are the same as if we had only a $(k - |O_v| + 1)$-pole with a single outer edge incident with v, since edges in O_v will be adjacent in all reachable basic k-poles. In other words, we can ignore the edge multiplicities when selecting the vertex v. Let $v_1, v_2, \ldots, v_p$ be the distinct inner neighbors of v and $m_1, m_2, \ldots, m_p$ be the edge multiplicities of the corresponding edge groups between v and its inner neighbors. Even though separating v from G formally adds $m_1 + \cdots + m_p$ outer edges, each group of edges between v and a single inner neighbor is adjacent in all reachable basic k-poles, so we can treat them as a single edge. Similarly, let q be 1 if $|O_v| > 0$ and 0 otherwise. We can then select the vertex v with the lowest value of $p - q$, as that is the value that truly reflects the possible growth of the multipole polynomial length. An example of this idea is shown in Figure 4.2.

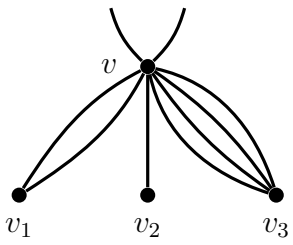

Figure 4.2: An example of edge groups. The outer edges are the upper ones; vertices v_1, v_2, v_3 are the inner neighbors of v. The edge group counts are $p = 3$ and $q = 1$ in this case, despite the edge counts being $|I_v| = 7$ and $|O_v| = 2$.

Computation of small k-pole polynomials

In the algorithm description above, we reattach the vertex v to the basic k'-poles in phase 4 and then compute the multipole polynomials of the small k-poles in phase 5 (assembling these multipole polynomials results in the multipole polynomial of G). This can be done easily by directly using the recursive formula from Theorem 1.2 (effectively, applying the naive algorithm). There is, however, an elegant shortcut that can be taken. Let S be one of the small k-poles that emerge when reattaching the vertex v to the basic k'-poles. We want to compute the multipole polynomial of S. We know that the only inner edges of S are the edges I_v, arranged in p groups of parallel edges with multiplicities $m_1, \ldots, m_p$. Each basic k-pole that could be reached from S during the recursive computation according to Theorem 1.2 is identified by assigning contraction or deletion to each group of parallel edges: in each branch of the naive recursion, either all edges in the group are deleted, or at least one of them is contracted (thus contracting the entire group).

Let $M \subseteq \{1, 2, \ldots, p\}$ be the indices of the groups that are contracted in a particular basic k-pole. We would like to quickly compute the coefficient c_M that corresponds to the basic k-pole P_M identified by M that is contributed to the final multipole polynomial when processing S.

Suppose that the naive recursion processes the edges in a fixed order in each group. Groups $i \notin M$ have all their edges deleted; in groups $i \in M$, there are some edges deleted first, then a single one is contracted, and the rest are treated as loops, i.e. they multiply the emerging coefficient value by 3 each (as per the first case in Theorem 1.2). Each branch of the naive recursion that reaches P_M is thus identified by a sequence of values ℓ_i for $i \in M$ such that $0 \leq \ell_i < m_i$, where ℓ_i is the number of loops created by the edges in the group i. If $L = \sum_{i \in M} \ell_i$, then the branch contributes to the coefficient c_M by 3^L. However, we must also account for the sign of the contribution, which is determined by the parity of the number of deletions. If the number of deletions is even, the branch is counted as positive; otherwise, it is negative (because the branch is reached by hitting the negative term in Theorem 1.2 an odd number of times). So the sign is determined by the parity of $D + D'$, where $D = \sum_{i \in M} m_i - 1 - \ell_i$ is the number of deletions in the groups that are contracted, and $D' = \sum_{i \notin M} m_i$ is the number of deletions in the groups that are deleted entirely. Note that $L + D + D' = (\sum_{i \in M} m_i - 1) + (\sum_{i \notin M} m_i) = |I_v| - |M|$ is not dependent on the specific branch.

All in all, the value of c_M can be expressed as:

$$c_M = \sum_{\substack{0 \leq \ell_i < m_i \\ \forall i \in M}} (-1)^{D+D'} 3^L = \sum_{\substack{0 \leq \ell_i < m_i \\ \forall i \in M}} (-1)^{L+D+D'} (-3)^L = (-1)^{|I_v|-|M|} \sum_{\substack{0 \leq \ell_i < m_i \\ \forall i \in M}} (-3)^L$$

We can notice that the sum can be gradually rearranged by always selecting an index

$j \in M$ and factoring out the terms corresponding to j according to the rule

$$\sum_{\substack{0 \le \ell_i < m_i \\ \forall i \in M}} (-3)^L = \left(\sum_{\ell_j=0}^{m_j-1} (-3)^{\ell_j} \right) \sum_{\substack{0 \le \ell_i < m_i \\ \forall i \in M-\{j\}}} (-3)^{L'},$$

where $L' = \sum_{i \in M-\{j\}} \ell_i$. This can be repeated until all terms are factored out, and we obtain:

$$c_M = (-1)^{|I_v|-|M|} \prod_{j \in M} \left(\sum_{\ell_j=0}^{m_j-1} (-3)^{\ell_j} \right) = (-1)^{|I_v|-|M|} \prod_{j \in M} \frac{1-(-3)^{m_j}}{1-(-3)}$$

Therefore, the value c_M that S contributes to the coefficient of P_M in the final multipole polynomial of G for the given M can be computed in time roughly linear in $|M|$. Given that computing the basic k-pole P_M is linear in $|M|$ anyway, we can consider this method optimal. If there are many parallel edges, this is significantly faster than iterating over all possible branches of the naive recursion. Of course, this improvement is not advantageous for cubic planar multipoles without parallel edges, but it shows that the algorithm can benefit from advanced optimizations in general.

Early return

Moreover, there are several situations where we can eliminate unnecessary computation: As we observed several times already, a non-proper multipole (a multipole with a degree-one inner vertex) has all coefficients equal to zero. In the sequential as well as the naive algorithm, there are situations where we can detect this easily and return zero without further computation. This can be the case for the k-pole G several steps into the algorithm execution, but also for the basic k-poles that emerge as the computation's base cases.

4.3 Implementation

We implemented both algorithms in the `C++` programming language. The source code can be found in Appendix A. We strived for a clean object-oriented implementation, with a reasonable focus on performance. Given the exponential nature of the problem, we focused on the algorithmic aspect of the computation over linear performance optimizations. Our implementation is able to handle also non-cubic and non-planar multipoles, but we will focus on cubic planar multipoles in the performance comparison.

In our implementation, we represent the outer vertices by negative integers and the inner vertices by non-negative integers. Edges incident to a vertex are stored as a multiset of neighbor vertices. The whole k-pole is then represented as an adjacency

list—in a map from vertices to their incident edges. This representation is efficient for our use case (sparse multipoles) and allows for easy local manipulation of a multipole, such as contracting or deleting an edge.

A basic k-pole can be elegantly represented as a set of sets of integers, where each set represents a group of adjacent outer vertices. For example, the basic 5-pole $B_1^{(5)}$ can be represented uniquely as $\{\{-5,-1\},\{-2,-3,-4\}\}$. A multipole polynomial is thus represented as a map from such basic k-poles to integer coefficients.

Regarding the data structures, `set` and `map` from the `C++` standard library can be used. However, since we are working with relatively small collections (sparse multipoles with up to a few tens of vertices), storing the data in flat arrays may be slightly more efficient. The `boost::container::flat_set` (and others) from the Boost library can be utilized for this purpose. We organized the source code so that it is easy to switch between the different container types. Our experimentation showed that there are indeed some measurable performance differences, but they are not great and not conclusive (for example, one container type may slightly speed up the computation at the expense of higher memory consumption). We selected reasonable default containers for each data structure in the final version of the implementation.

We also added basic integration tests: Randomly generated dense multipoles, as well as many cubic planar multipoles, are fed to both algorithms and compared against each other, and also against our reference implementation of the naive algorithm in Python. Given that the multipole polynomial coefficients may have a large magnitude, there is a risk that we could encounter an integer overflow during the computation, which would lead to incorrect results. We used the `-fsanitize=signed-integer-overflow` compiler option that aborts the computation if an overflow is detected. This option is inexpensive performance-wise and if the computation finishes without an error, we can be decently confident that the results are correct.

The implementation supports two input formats—either a list of vertex number pairs representing the edges (enumerated on the standard input in text form); or the binary *planar code* used by the `plantri` software described in the following section. Our tool can provide several different outputs, most notably a string representation of the multipole polynomial, and a condensed sequence of coefficient values for small values of k.

4.4 Cubic planar multipole generation

To compare the performance of the algorithms as well as to compute the coefficient values for the analysis in Chapter 5, generating all cubic planar multipoles of a given size is critical. Fortunately, there is an efficient tool `plantri` [16] capable of generating

several different classes of planar graphs. When provided the option `-P`, `plantri` generates triangulations of a disk. When the option `-d` is added, the dual graphs are returned instead. The outer face of the disk corresponds to a vertex in the dual graph. If we interpret this vertex as a union of the outer vertices of a multipole, the dual graph to a disk triangulation with the perimeter containing k vertices exactly corresponds to a cubic planar k-pole. We can specify the total number of vertices and optionally the number of outer vertices k to generate. We will denote the number of inner vertices n and the total number of vertices $v = n + k$. Since every edge is shared by two vertices and each vertex in a cubic multipole has an odd degree, v has to be even.

In the primal context, all non-isomorphic disk triangulations without loops, without parallel edges and with each inner vertex degree of at least 3 are generated by `plantri`. What cubic planar multipoles are we omitting by these restrictions? A loop corresponds to a trivial bridge in the dual multipole, so no trivial bridges will be present. A pair of parallel edges in a triangulation determines a portion of the dual multipole that forms a smaller 2-pole. As noted in Chapter 3, such a 2-pole poses only as a multiplicative constant to all multipole polynomial coefficients of the rest of the multipole (where the 2-pole is replaced by a regular inner edge). We are therefore free to ignore the omission of such multipoles by `plantri`. Similarly, if an inner vertex in the primal triangulation had a degree of 2, it would correspond to a pair of parallel edges in the dual cubic multipole, which can be ignored for the same reason.

By default, `plantri` generates only triangulations without chords and without degree-two vertices on the disk perimeter. Chords correspond to non-trivial bridges in the multipole, which means that if we want to allow them, we need to provide the option `-c2`. A degree-two vertex on the disk perimeter translates to a pair of adjacent outer edges in the cubic multipole; we can allow them by the option `-m2`. A pair of adjacent outer edges also necessitates a non-trivial bridge (the single inner edge incident with the pair). For that reason, `-m2` requires also the `-c2` option.

Since the primal graph is a triangulation of the disk, the dual graph is connected. Supplying the options `-c2m2dP` thus generates all connected cubic planar multipoles without trivial bridges and the non-interesting embedded 2-poles. Adding the option `-u` instructs `plantri` to return only the count of the multipoles that would otherwise be generated. This way, we determined the numbers of the generated k-poles for small values of k and v, as shown in Table 4.1 and Table 4.2. We can see that the number of multipoles grows exponentially with the number of vertices, as one would expect.

Finally, `plantri` provides the `res/mod` functionality: If we supply integer values for the `res` and `mod` parameters, the program will split all the graphs into `mod` classes in a roughly uniform manner and generate only the `res`-th class. This is useful for easy parallelization of the computation if we want to compute the multipole polynomial coefficients for a large number of multipoles.

v	$k=3$	$k=4$	$k=5$	$k=6$	$k=7$	all
4	0					0
6	1	0				1
8	1	1	0			2
10	4	2	1	0		7
12	16	8	2	1	0	27
14	78	38	12	3	1	132
16	457	219	73	20	3	773
18	2938	1404	503	140	27	5017
20	20118	9714	3661	1089	235	34861
22	144113	70454	27715	8796	2149	253676
24	1065328	527235	214664	72204	19419	1903584
26	8068332	4037671	1691049	596906	173779	14616442
28	62297808	31477887	13494718	4958736	1538221	114254053
30	488755938	249026400	108864742	41365110	13516342	906266345
32	3886672165	1994599707	886520081	346477770	118196961	7277665889
34	31269417102	16147744792	7279644889	2914165157	1030817669	59066524810

Table 4.1: Numbers of k-poles generated by `plantri -dP`.

v	$k=3$	$k=4$	$k=5$	$k=6$	$k=7$	all
4	1					1
6	1	1				2
8	1	2	1			4
10	4	5	4	3		16
12	16	18	14	11	4	63
14	78	88	69	53	28	328
16	457	489	396	295	178	1933
18	2938	3071	2503	1867	1196	12633
20	20118	20667	16905	12560	8385	87466
22	144113	146381	119571	89038	60736	633015
24	1065328	1072760	874771	652198	451613	4717745
26	8068332	8071728	6567181	4903955	3429943	35980100
28	62297808	61990477	50329363	37627699	26513787	279418926
30	488755938	484182622	392328944	293607612	208049054	2202903618
32	3886672165	3835654678	3102523829	2323604832	1653791089	17590599410
34	31269417102	30757242535	24839151315	18614121391	13295553654	142025760202

Table 4.2: Numbers of k-poles generated by `plantri -c2m2dP`.

4.5 Performance comparison

We evaluated the performance of both algorithms on all cubic planar multipoles generated by `plantri -c2m2dP` for $16 \leq v \leq 24$ on a personal computer. We performed five measurements for each v and algorithm; they turned out to be very consistent (the standard deviation always being within a few percent). The mean values across the five runs are reported in Table 4.3. For each value v and algorithm, we list the total computation time for all the multipoles of the given size; the average time for a single multipole; and the maximum memory consumption for the given set of multipoles.

		naive algorithm			sequential algorithm		
v	multipoles	total time	avg. time	max mem.	total time	avg. time	max mem.
16	1933	1.07 s	0.554 ms	2720 kB	0.08 s	0.041 ms	2048 kB
18	12633	12.04 s	0.953 ms	3968 kB	0.75 s	0.059 ms	2080 kB
20	87466	140.72 s	1.609 ms	6592 kB	7.45 s	0.085 ms	2080 kB
22	633015	1639.39 s	2.590 ms	12512 kB	75.59 s	0.119 ms	2080 kB
24	4717745	19212.53 s	4.072 ms	26104 kB	780.46 s	0.165 ms	2112 kB

Table 4.3: Comparison of computation time and required memory for both algorithms. Each row is the average of five (rather similar) measurements.

The base memory allocated by any execution of our program was usually 2080 kilobytes. It makes sense to subtract the base memory from the total memory consumption when extrapolating the memory requirements for larger multipoles. This *adjusted* memory consumption as well as the multipole count and total computation time is displayed on a logarithmic scale in Figure 4.3. We also calculated the exponential regression for the data points, displayed in the plots as well. We can observe that with each step of v, the multipole count grows by a factor of approximately 7.54, the total computation time of the naive algorithm by a factor of approximately 15.1, and the total computation time of the sequential algorithm by a factor of approximately 11.7—the sequential algorithm thus appears to be asymptotically faster than the naive algorithm. Moreover, the adjusted maximum memory consumption of the naive algorithm grows by a factor of approximately 2.39, which means that for v somewhere between 30 and 40, there will likely be multipoles that require several gigabytes of memory to process. On the other hand, the maximum memory consumption of the sequential algorithm was hardly distinguishable from the base memory (therefore not displayed in the plot). Even though it is very likely that the memory consumption would increase with higher values of v, we believe it is reasonable to conclude that one might encounter multipole classes that are difficult to process with the naive algorithm, while the sequential algorithm should be able to handle them more easily.

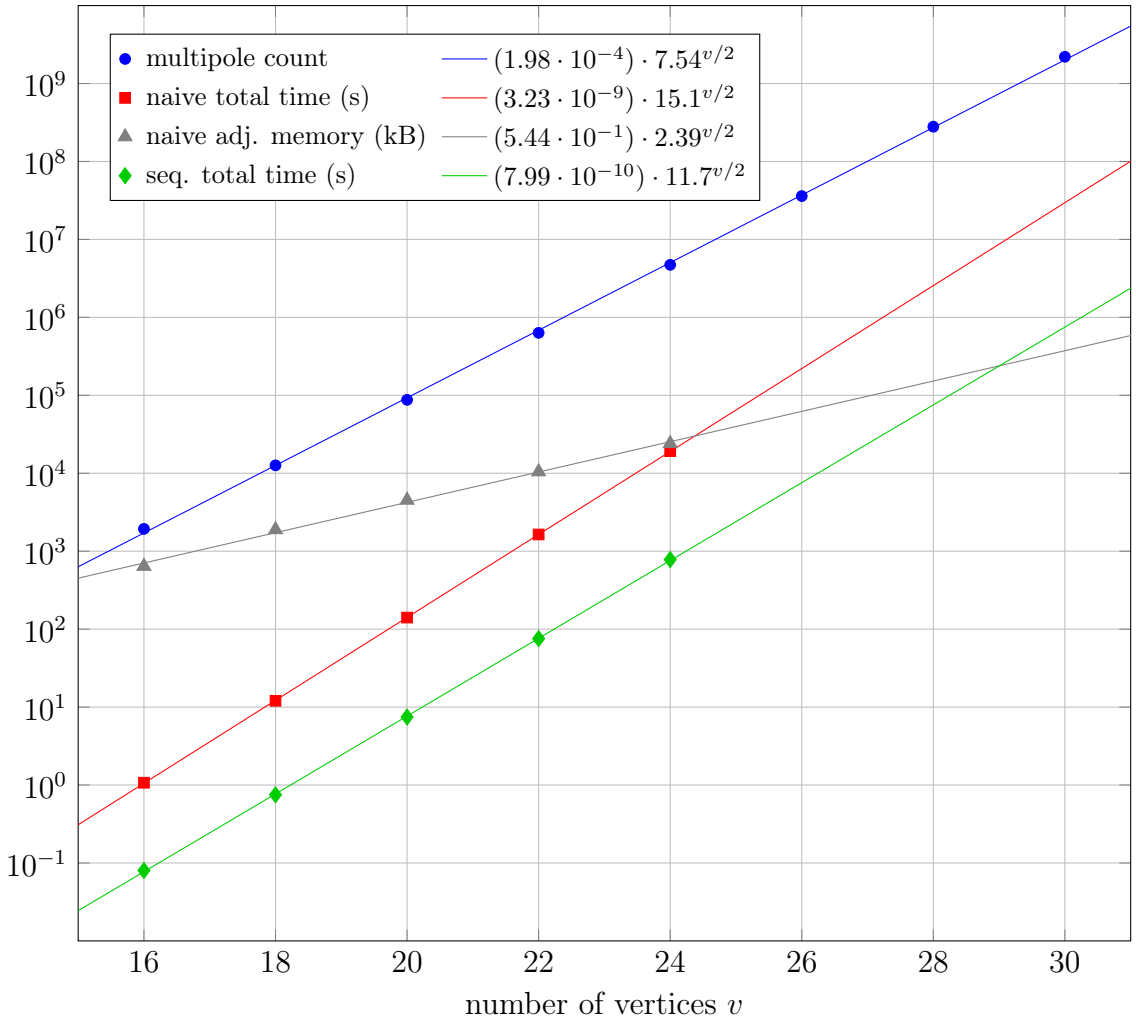

Figure 4.3: Algorithm performance comparison on a logarithmic scale. The lines show the exponential regression for the data points. The sequential algorithm memory consumption is not displayed due to its minuscule magnitude.

Although this brief comparison does not aim to provide an exhaustive performance analysis, it is evident that significant performance improvements can be achieved by employing more sophisticated methods, such as the sequential approach. It is worth noting that removing the vertex selection heuristic described in Section 4.2 does significantly decrease the algorithm's performance, so it is indeed crucial to the algorithm's effectiveness.

Chapter 5

Empirical value constraints

Utilizing the `C++` implementation of the sequential algorithm described in Chapter 4, we computed the multipole polynomial coefficients for small k-poles for $k \in \{4, 5, 6\}$. The computed data are attached in Appendix A. We will analyze them in the following sections.

5.1 4-pole constraints

As described multiple times in this work, we know that every cubic planar 4-pole must obey the following constraints corresponding to the non-negativity of flow counts with a given boundary:

$$\begin{aligned} a + b_1 + b_2 &\geq 0 && \text{(T1)} \\ a + b_1 &\geq 0 && \text{(T2)} \\ a + b_2 &\geq 0 && \text{(T3)} \\ a &\geq 0 && \text{(T4)} \end{aligned}$$

We will call these constraints *theoretical*. We aim to find out whether the real 4-poles satisfy them tightly, or whether there are some more strict linear constraints that the real 4-poles obey—we will call those *empirical* constraints. For this purpose, we computed the coefficients for all 4-poles generated by `plantri -c2m2dP` for $v \leq 30$. Each 4-pole can be thought of as a point in the three-dimensional space spanned by the coefficients a, b_1, b_2. Since the coefficients b_1 and b_2 are symmetric to an extent, we can plot the value of $b_1 + b_2$ against a for each 4-pole. The resulting scatter plot is shown in Figure 5.1. Constraints T4 and T1 are displayed in cyan and magenta, respectively. The sum of constraints T2 and T3, $2a + (b_1 + b_2) \geq 0$, could be displayed as well, but it is dominated by T1 and T4 which are more strict than the combination of T2 and T3.

An elegant way to discover empirical constraints in general higher-dimensional spaces is to use the convex hull: If we compute the convex hull of the points corresponding to

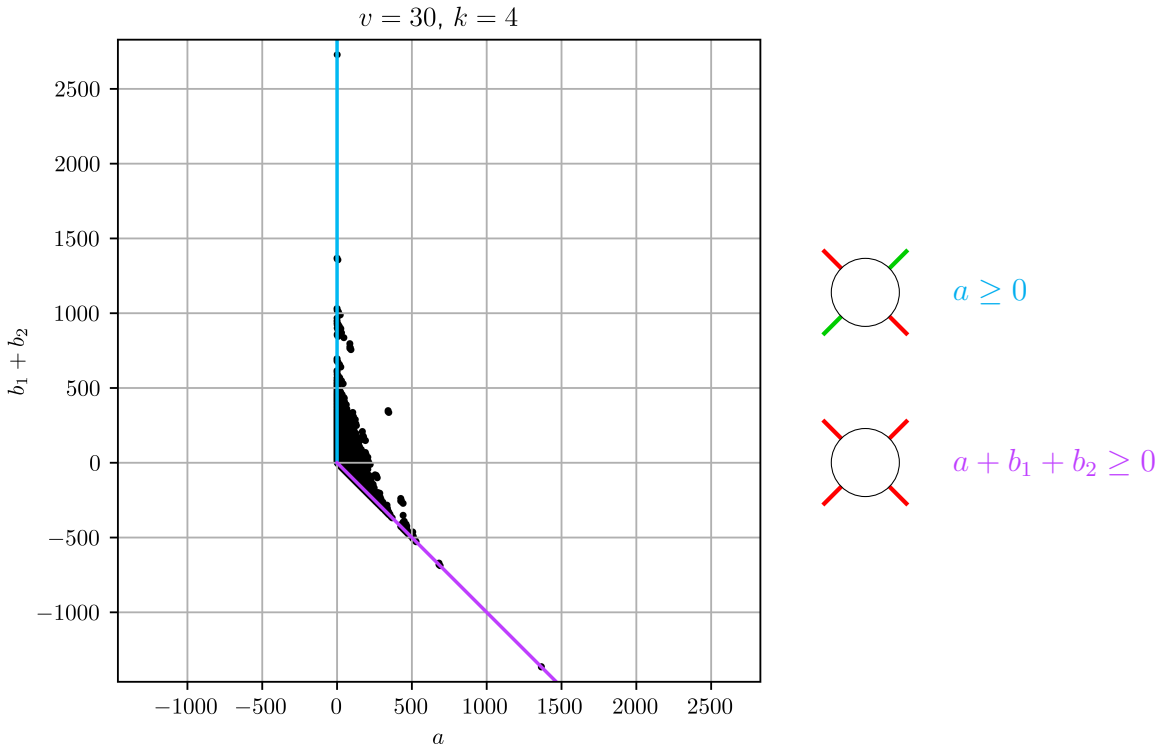

Figure 5.1: Empirical constraints for 4-poles.

the 4-poles and select the facets of the hull that contain the origin, we obtain the linear inequalities that are satisfied by all 4-poles. We did this for the 4-poles with $v \leq 30$ and the resulting empirical constraints turned out to exactly match the theoretical constraints T1 to T4. The same result is obtained if we limit ourselves to 4-poles without any bridges, generated by `plantri -dP`. The code used for this computation is available in Appendix A.

Finally, we can briefly observe some of the classes of 4-poles that secure the tightness of the theoretical constraints. The two points in Figure 5.1 near the cyan and magenta lines far away from the origin correspond to the *ladder* 4-pole and the *modified ladder* 4-pole, as illustrated in Figure 5.2.

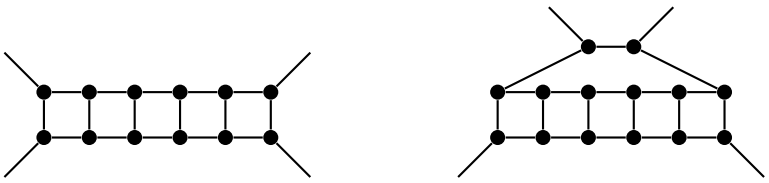

$a = 0,\ b_1 = 21,\ b_2 = 1$ $\qquad$ $a = 21,\ b_1 = -21,\ b_2 = 2$

Figure 5.2: The ladder and the modified ladder 4-poles.

By determining the flow counts $f_\beta(G)$ for these two 4-poles, it can be shown that for v divisible by four, the ladder has $a = 0$, $b_2 = 1$, and b_1 growing exponentially with v.

This means that with increasing v, the point (a, b_1, b_2) gets arbitrarily far from the origin while still having $a = 0$ and $a + b_2 = 1$, thus making the constraints T4 and T3 (and T2 by rotation) tight. Similarly, for v of the form $4v' + 2$, the modified ladder has $b_2 = 2$, and $a = -b_1$ growing exponentially with v. The point thus gets arbitrarily far from the origin while having $a + b_1 + b_2 = 2$ (i.e. in a constant distance from the plane $a + b_1 + b_2 = 0$), making the constraint T1 tight.

The same 4-poles serve as examples of the tightness of the constraints for the $(2, 2)$-connectivity and $(2, 2)$-2-connectivity examined in Chapter 3. The *rotated* ladder is $(2, 2)$-connected, but it has the indicator value $I = 2a+b_1 = 2\cdot 0+1 = 1$, being ultimately close to the $I > 0$ criterion for $(2, 2)$-connectedness. Similarly, the *rotated* modified ladder is $(2, 2)$-2-connected and yet has the indicator value $J = 2a+b_1+2b_2 = 2a+2+2\cdot(-a) = 2$ rather close to the $J > 0$ criterion. If we project the points to the coordinates given by the indicators I and J, the two 4-poles then reside in the immediate vicinity of the two inequalities $I > 0$ and $J > 0$ backed by the Four color theorem, as shown in Figure 5.3, thus satisfying the constraints tightly.

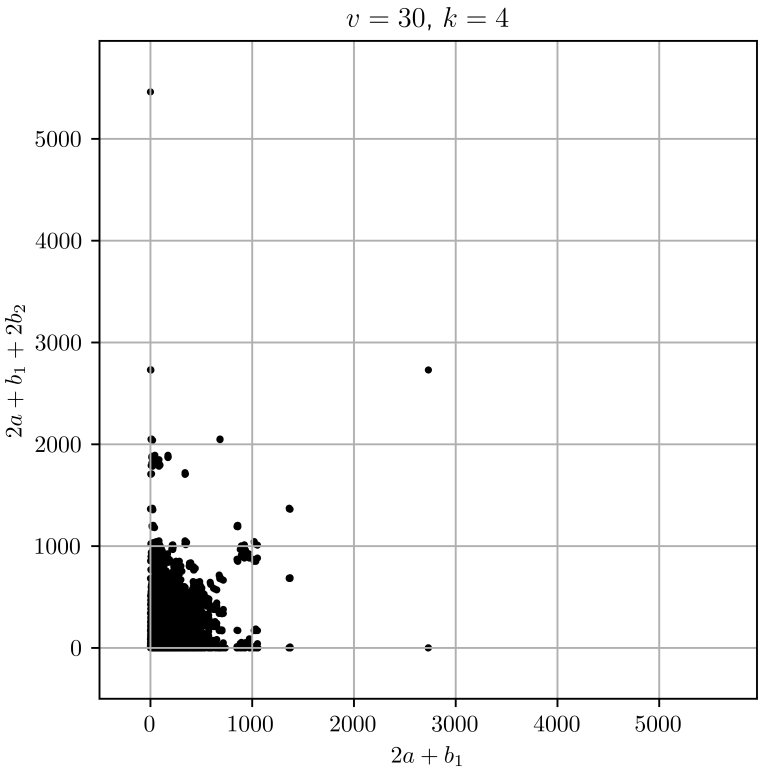

Figure 5.3: Projection of the 4-pole coefficients to the base given by I and J.

5.2 5-pole constraints

There are 10 admissible boundaries for planar 5-poles, as listed in Figure 1.2. The boundary `11213` is compatible with basic 5-poles $A^{(6)}$ and $B_2^{(6)}$. The boundary `11123` is compatible with $A^{(6)}$, $B_2^{(6)}$ and $B_3^{(6)}$. Therefore, the five rotations of `11213` yield the theoretical constraints T1 to T5, and the five rotations of `11123` are responsible for the theoretical constraints T6 to T10:

$$\begin{aligned} a + b_1 &\geq 0 \quad \text{(T1)} & a + b_1 + b_2 &\geq 0 \quad \text{(T6)} \\ a + b_2 &\geq 0 \quad \text{(T2)} & a + b_2 + b_3 &\geq 0 \quad \text{(T7)} \\ a + b_3 &\geq 0 \quad \text{(T3)} & a + b_3 + b_4 &\geq 0 \quad \text{(T8)} \\ a + b_4 &\geq 0 \quad \text{(T4)} & a + b_4 + b_5 &\geq 0 \quad \text{(T9)} \\ a + b_5 &\geq 0 \quad \text{(T5)} & a + b_1 + b_5 &\geq 0 \quad \text{(T10)} \end{aligned}$$

For the sake of brevity, we will denote $b = b_1 + b_2 + b_3 + b_4 + b_5$. By summing the constraints T1 to T5 and T6 to T10, respectively, we obtain the following summary theoretical constraints:

$$5a + b \geq 0 \quad \text{(T1}') \qquad\qquad 5a + 2b \geq 0 \quad \text{(T2}')$$

Similarly to the previous section, we computed the coefficients for all 5-poles generated by `plantri -c2m2dP` for $v \leq 30$. The scatter plot of b against a is shown in Figure 5.4. The constraints T1′ and T2′ are displayed in cyan and magenta, respectively. In contrast to the 4-pole case, the points here appear to be restricted also by an additional constraint, $2a + b \geq 0$, displayed in yellow (rendering the constraint T2′ superfluous).

Utilizing the convex hull method to discover the empirical constraints for the points in the original, six-dimensional space, we found that eleven linear inequalities are satisfied by all 5-poles: Ten of them match the theoretical constraints T1 to T10, and the additional constraint E1 is $2a + b_1 + b_2 + b_3 + b_4 + b_5 \geq 0$, indeed. Furthermore, we computationally verified that this constraint is satisfied by all more than $2.4 \cdot 10^{10}$ 5-poles with $v \leq 34$ generated by `plantri -c2m2dP`. Again, the same empirical constraints are obtained for 5-poles without bridges, generated by `plantri -dP`. This leads us to the following hypothesis:

Hypothesis 5.1. Every cubic planar 5-pole satisfies $2a + b \geq 0$.

Note that this hypothesis can be reformulated as follows: Denote $f^{\circlearrowleft}_{\texttt{11213}}(G)$ the sum of $f_\beta(G)$ over the rotations β of the boundary `11213`, and $f^{\circlearrowleft}_{\texttt{11123}}(G)$ the sum of $f_\beta(G)$ over the rotations β of the boundary `11123`. Then $f^{\circlearrowleft}_{\texttt{11213}}(G) = 5a + b$ and

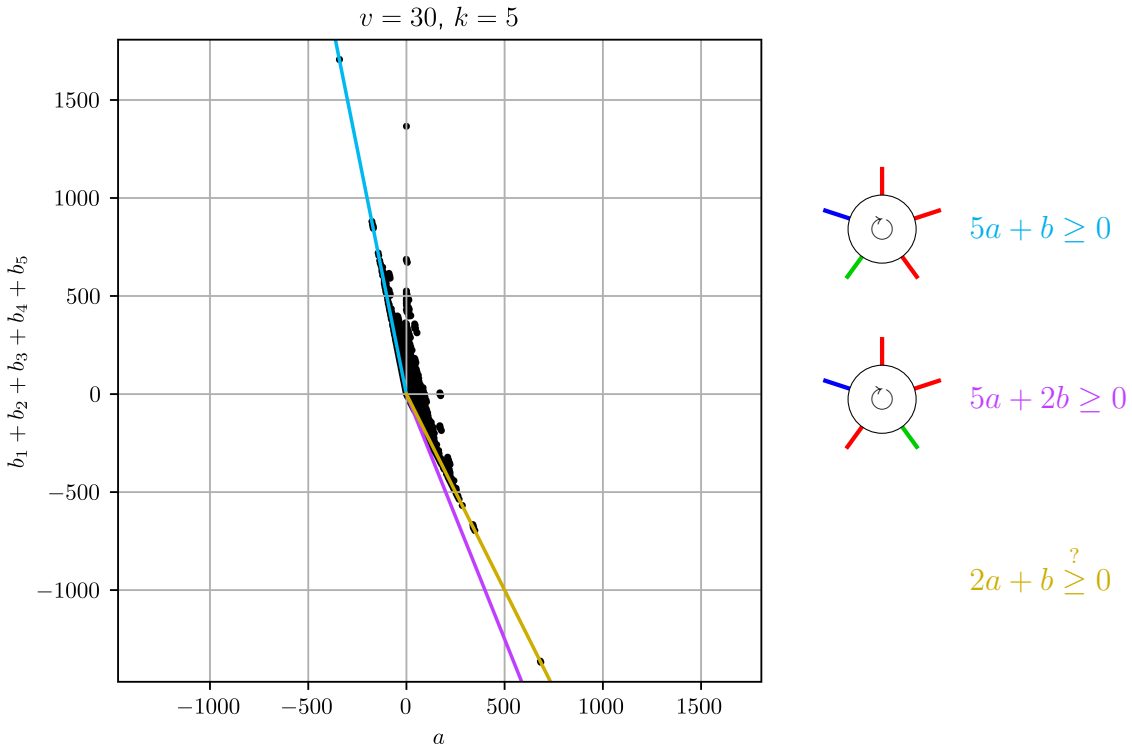

Figure 5.4: Empirical constraints for 5-poles.

$f^{\circlearrowleft}_{\texttt{11123}}(G) = 5a + 2b$. It can be noticed that

$$5a + 2b = \frac{1}{3}(5a + b) + \underbrace{\frac{5}{3}(2a + b)}_{\overset{?}{\geq}0},$$

so if the hypothesis holds, then $f^{\circlearrowleft}_{\texttt{11123}}(G) \geq \frac{1}{3} f^{\circlearrowleft}_{\texttt{11213}}(G)$ for every 5-pole G.

The angle between constraints E1 and T2′ in Figure 5.4 thus translates to a statement about colorings count ratio: At least a quarter of the total number of colorings of a 5-pole must have the boundary `11123` or its rotation. In a sense, this can be viewed as a somewhat stronger statement than the Four color theorem: If a cubic planar 5-pole G without trivial bridges had no colorings with one of the `11123` boundaries, we could extend it by a 5-cycle to a bridgeless cubic planar graph H' (like in Chapter 3) and since the extension is only compatible with `11123` boundaries, H' would be a planar snark. The Four color theorem thus implies that if G has flows, it has at least one flow of the `11123` type. On the other hand, Hypothesis 5.1 states that the number of such flows is at least a quarter of the total number of flows.

5-pole hypothesis counterexample properties

In order to examine the plausibility of Hypothesis 5.1, we will investigate the properties that an eventual counterexample would have to possess, in addition to the computations

for small 5-poles performed above. Let G be the smallest cubic planar 5-pole that does not satisfy Hypothesis 5.1.

Lemma 5.1. *G is connected.*

Proof. Suppose that G is disconnected. There must exist a rotation of G and numbers p, r such that the rotation is (p, r)-disconnected. Then (p, r) equals either $(0, 5)$, $(1, 4)$, or $(2, 3)$. As we showed in Chapter 3, if G is $(0, 5)$-disconnected, the 0-pole component serves only as a multiplicative factor to the coefficients of the other part G'. Therefore, G' would also be a counterexample to the hypothesis, which contradicts the minimality of G. If G is $(1, 4)$-disconnected instead, the 1-pole component does not contain a flow by Lemma 1.1, so the entire G does not contain a flow. Because of this, $f^{\circlearrowleft}_{11123}(G) = f^{\circlearrowleft}_{11213}(G) = 0$, and $f^{\circlearrowleft}_{11123}(G) \geq \frac{1}{3} f^{\circlearrowleft}_{11213}(G)$ holds, so G satisfies the hypothesis.

Finally, suppose that G is $(2, 3)$-disconnected. The flows in the 2-pole G' and 3-pole G'' (that form the components of G) are independent, so let $a' \cdot f_{\beta'}(A^{(2)})$ and $a'' \cdot f_{\beta''}(A^{(3)})$ be the multipole polynomials of G' and G'', respectively. As per Lemma 1.1, each flow in G must assign the same value to the two outer edges of G' and the three different values to the outer edges of G''. Therefore, we can directly enumerate the flow counts of G:

$$
\begin{aligned}
f_{11213}(G) &= a'a'' & f_{11123}(G) &= a'a'' \\
f_{12131}(G) &= 0 & f_{11231}(G) &= a'a'' \\
f_{21311}(G) &= 0 & f_{12311}(G) &= 0 \\
f_{13112}(G) &= 0 & f_{23111}(G) &= 0 \\
f_{31121}(G) &= 0 & f_{31112}(G) &= 0
\end{aligned}
$$

In total, $f^{\circlearrowleft}_{11213}(G) = a'a''$ and $f^{\circlearrowleft}_{11123}(G) = 2 \cdot a'a''$, so $f^{\circlearrowleft}_{11123}(G) = 2 f^{\circlearrowleft}_{11213}(G) \geq \frac{1}{3} f^{\circlearrowleft}_{11213}(G)$ and G satisfies the hypothesis, which is again a contradiction. □

Lemma 5.2. *G contains no inner edge that is a bridge.*

Proof. Suppose that G contains an inner edge that is a bridge. By the same logic as above, the bridge is either a $(0, 5)$-bridge, a $(1, 4)$-bridge, or a $(2, 3)$-bridge in one of the rotations of G. In the first case, we showed in Chapter 3 that G would have all coefficients equal to zero, which satisfies the hypothesis. We also showed that a $(1, 4)$-bridge separates a 2-pole from a 5-pole, and the 2-pole serves only as a multiplicative factor to the coefficients of the 5-pole, which contradicts the minimality of G.

In the last case, the bridge separates a 3-pole G' from a 4-pole G''. Let their multipole polynomials be $a' \cdot f_{\beta'}(A^{(3)})$ and $a'' \cdot f_{\beta''}(A^{(4)}) + b''_1 \cdot f_{\beta''}(B^{(4)}_1) + b''_2 \cdot f_{\beta''}(B^{(4)}_2)$, respectively. Each flow in G must assign exactly the three different values to the outer

edges of G', so we can deduct the value assigned to the bridge for any given boundary of G (if one exists). Therefore, the flow counts of G are:

$$f_{11213}(G) = 0 \qquad f_{11123}(G) = 0$$
$$f_{12131}(G) = a' \cdot f_{3131}(G'') = a'a'' \qquad f_{11231}(G) = 0$$
$$f_{21311}(G) = a' \cdot f_{3311}(G'') = a'(a'' + b_2'') \qquad f_{12311}(G) = a' \cdot f_{3311}(G'') = a'(a'' + b_2'')$$
$$f_{13112}(G) = a' \cdot f_{2112}(G'') = a'(a'' + b_1'') \qquad f_{23111}(G) = a' \cdot f_{1111}(G'') = a'(a'' + b_1'' + b_2'')$$
$$f_{31121}(G) = a' \cdot f_{2121}(G'') = a'a'' \qquad f_{31112}(G) = a' \cdot f_{2112}(G'') = a'(a'' + b_1'')$$

This gives us $f^{\circlearrowleft}_{11213}(G) = a'(4a'' + b_1'' + b_2'')$ and $f^{\circlearrowleft}_{11123}(G) = a'(3a'' + 2b_1'' + 2b_2'')$. We know that G' satisfies $a' \geq 0$ and G'' satisifies $a'' + b_1'' + b_2'' \geq 0$. Thus we get $3f^{\circlearrowleft}_{11123}(G) = a'(9a'' + 6b_1'' + 6b_2'') \geq a'(9a'' + 6b_1'' + 6b_2'') - 5a'(a'' + b_1'' + b_2'') = a'(4a'' + b_1'' + b_2'') = f^{\circlearrowleft}_{11213}(G)$. As a result, $f^{\circlearrowleft}_{11123}(G) \geq \frac{1}{3} f^{\circlearrowleft}_{11213}(G)$ and G satisfies the hypothesis, which is a contradiction. □

Lemma 5.3. *If G contains a pair of inner edges e_1, e_2 that would make G disconnected if removed, then both e_1 and e_2 are adjacent to the same outer edge.*

Proof. Suppose that G contains a pair of inner edges e_1, e_2 that would make G disconnected if removed, such that they are not adjacent to the same outer edge. The edges e_1, e_2 form either a $(0, 5)$-2-cut, a $(1, 4)$-2-cut, or a $(2, 3)$-2-cut in one of the rotations of G. If they form a $(0, 5)$-2-cut, they separate a 2-pole portion of G that poses only as a multiplicative factor, contradicting the minimality of G.

Suppose that e_1, e_2 form a $(1, 4)$-2-cut, separating a 3-pole G' from a 6-pole G''. If G' consisted only of a single inner vertex, e_1 and e_2 would be adjacent to a common outer edge. Therefore, G' must be larger. Let us construct G_1: a smaller version of G where G' is replaced by a single inner vertex. By minimality of G, we know that G_1 must satisfy the hypothesis. However, if $a' \cdot f_{\beta'}(A^{(3)})$ is the multipole polynomial of G', then the coefficients of G are a'-multiples of the coefficients of G_1 (because the flows inside G' for a given boundary of G' are independent of the rest of G), which implies that G satisfies the hypothesis, contradicting the premise.

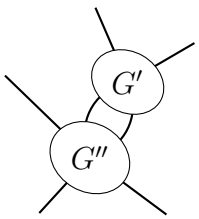

Figure 5.5: A diagram of a $(2, 3)$-2-cut in a 5-pole.

Finally, suppose that e_1, e_2 form a $(2, 3)$-2-cut, separating a 4-pole G' from a 5-pole G'', like in Figure 5.5. This is the most challenging case, and for the sake of

demonstration, we will take a slightly different approach—systematically computing the coefficients $(a, b_1, b_2, b_3, b_4, b_5)$ of G. Let (a', b'_1, b'_2) and $(a'', b''_1, b''_2, b''_3, b''_4, b''_5)$ be the coefficients of G' and G'', respectively. Imagine the recursive computation of the multipole polynomial of G where only the inner edges of G' are taken into account and G'' is not processed. We can see that the multipole polynomial of G is then equal to:

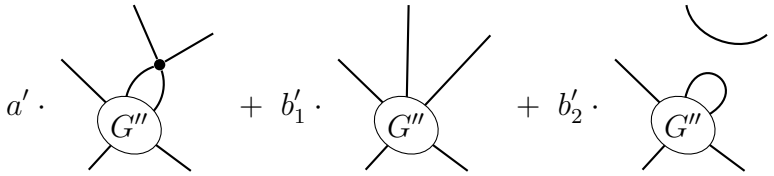

Subsequently, we can ignore the attached basic 4-poles and process only the inner edges of G''. This way, we will arrive at 18 small 5-poles (consisting of a basic 4-pole attached to a basic 5-pole), each multiplied by one coefficient of G' and one coefficient of G''. These small 5-poles can then be processed as usual:

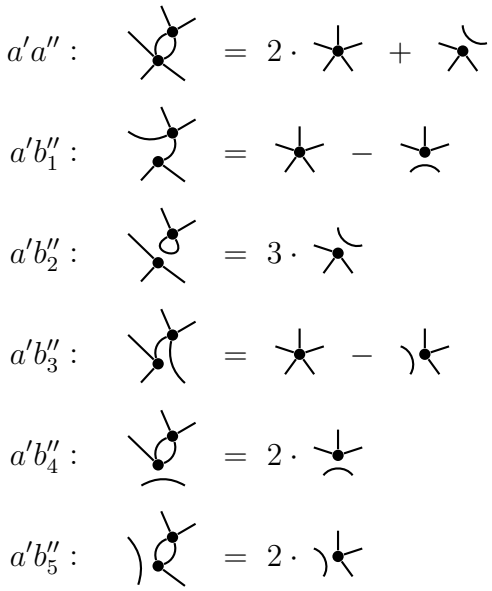

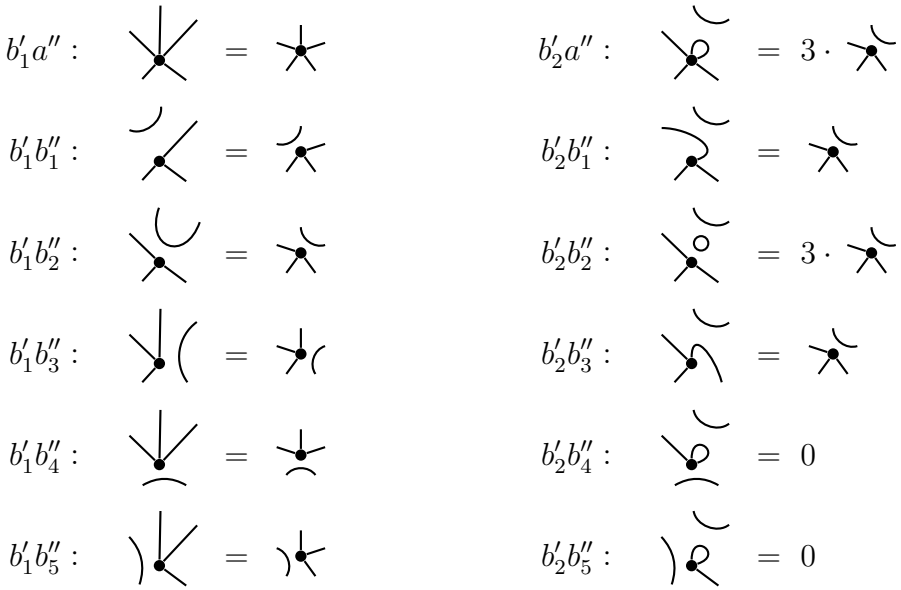

We can now assemble the coefficients of G:

$$\begin{aligned}
a &= 2a'a'' + a'b_1'' + a'b_3'' + b_1'a'' \\
b_1 &= b_1'b_1'' \\
b_2 &= a'a'' + 3a'b_2'' + b_1'b_2'' + 3b_2'a'' + b_2'b_1'' + 3b_2'b_2'' + b_2'b_3'' \\
b_3 &= b_1'b_3'' \\
b_4 &= -a'b_1'' + 2a'b_4'' + b_1'b_4'' \\
b_5 &= -a'b_3'' + 2a'b_5'' + b_1'b_5''
\end{aligned}$$

To reach a contradiction with the assumption that G is a counterexample to the hypothesis, we would like to prove that $2a + b \geq 0$. We have:

$$\begin{aligned}
2a + b_1 + b_2 + b_3 + b_4 + b_5 = & \\
&= 5a'a'' + \ a'b_1'' + 3a'b_2'' + \ a'b_3'' + 2a'b_4'' + 2a'b_5'' \\
&+ 2b_1'a'' + \ b_1'b_1'' + \ b_1'b_2'' + \ b_1'b_3'' + \ b_1'b_4'' + \ b_1'b_5'' \\
&+ 3b_2'a'' + \ b_2'b_1'' + 3b_2'b_2'' + \ b_2'b_3''
\end{aligned} \tag{5.1}$$

Suppose first that $b_2' \geq 0$. The expression in eq. (5.1) can be rearranged as follows:

$$\begin{aligned}
& a' \left(2(a'' + b_2'') + (a'' + b_4'' + b_5'')\right) \\
+ \ & (a' + b_1') \left(2a'' + b_1'' + b_2'' + b_3'' + b_4'' + b_5''\right) \\
+ \ & b_2' \left((a'' + b_1'' + b_2'') + (a'' + b_2'' + b_3'') + (a'' + b_2'')\right)
\end{aligned}$$

By the minimality of G, the smaller 5-pole G'' must satisfy the hypothesis, i.e. $2a'' + b'' \geq 0$. All the remaining terms are non-negative since they are equal to the theoretical constraints for 4-poles and 5-poles. Therefore, $2a + b \geq 0$ in this case, as desired.

On the other hand, suppose that $-b_2' \geq 0$. Combined with the theoretical constraint $a' \geq 0$, we get $a - b_2' \geq 0$. We can then rearrange the expression in eq. (5.1) as follows instead:

$$\begin{aligned}
& (a' + b_1' + b_2')(2a'' + b_1'' + b_2'' + b_3'' + b_4'' + b_5'') \\
+ \ & 2(a' + b_2')(a'' + b_2'') \\
+ \ & (a' - b_2')(a'' + b_4'' + b_5'')
\end{aligned}$$

Again, all the terms are non-negative, hence the entire expression is. This concludes the proof. □

Note that if we managed to prove the previous lemma even for pairs of edges adjacent to an outer edge, the hypothesis would obviously be proven as a whole, since every

outer edge is either adjacent to such a pair of inner edges, or to another outer edge and a $(2,3)$-bridge.

Putting together with the fact that we computationally verified the hypothesis for $v \leq 34$, we obtain the following result:

Theorem 5.1. *If Hypothesis 5.1 does not hold and G is its smallest counterexample, then for every p, r such that $p + r = 5$, every rotation of G is (p, r)-2-connected and contains no (p, r)-2-cuts except possibly the $(1, 4)$-2-cuts consisting of a pair of inner edges adjacent to the same outer edge. Moreover, G has at least 36 vertices.*

At least some of the results in this section could alternatively be proven using Kempe chains, similarly to the motivational example in Section 1.5. However, our approach highlights that the multipole polynomial coefficients are a powerful and natural tool for a task such as this.

5.3 6-pole constraints

Let us finish this chapter by examining the constraints for 6-poles. There are 31 admissible boundaries for 6-poles and 15 basic 6-poles (as shown in Figure 1.3). There are two issues with the growing numbers: The list of constraints becomes impractically long, and the 15 dimensions become too many for the standard convex hull algorithm to handle when discovering the empirical constraints. For these reasons, we will limit ourselves to the reduced space where we sum the coefficients that are equivalent under rotation. Let us denote $b = b_1 + b_2 + b_3 + b_4 + b_5 + b_6$, $c = c_1 + c_2 + c_3$, $d = d_1 + d_2 + d_3$, and $e = e_1 + e_2$. If we compute the coordinates a, b, c, d, e of each 6-pole in the 5-dimensional space, we see that the same coordinates are obtained for all rotations of the 6-pole. Alternatively, we can view this dimension reduction as summing the original coefficient values over the 6 rotations of the 6-pole—this way, all coefficient values corresponding to basic 6-poles that are equivalent under rotation will reach the same value, serving as a single coordinate in the reduced space.

We have computed the coordinates in the reduced space for all 6-poles generated by `plantri -c2m2dP` for $v \leq 34$. The 9 theoretical constraints given by the admissible boundaries as well as the 10 discovered empirical constraints are listed in Table 5.1. Analogously to the constraints listed in the previous sections, each row corresponds to a linear inequality given by the non-negativeness of the flow count for a given boundary and its rotations. For example, the second row states that every 6-pole G must satisfy $f^{\circlearrowleft}_{111212}(G) = 6a + 2b \geq 0$.

The seven theoretical constraints T1 to T7 match the seven empirical constraints E1 to E7. Theoretical constraints T8 and T9 were not discovered as empirical; instead, three more empirical constraints E8 to E10 were found. The reason why T8 and T9

$\circlearrowleft \beta$	a	b	c	d	e	constraint
111111	1	1	0	1	1	T1 = E1
111212	6	2	0	0	0	T2 = E2
112112	3	1	0	1	0	T3 = E3
112233	2	1	0	0	1	T4 = E4
112332	3	1	1	1	0	T5 = E5
121323	3	0	2	0	0	T6 = E6
123123	1	0	1	0	0	T7 = E7
111122	6	4	0	2	3	T8
112323	6	1	2	0	0	T9
	4	2	0	0	1	E8
	4	2	1	1	1	E9
	9	3	2	1	3	E10

Table 5.1: Theoretical and empirical constraints for 6-poles.

were not discovered is that they can be expressed as a combination of other empirical constraints—E1 and E8, or E2 and E6, respectively:

$$(6,4,0,2,3) = 2 \cdot (1,1,0,1,1) + 1 \cdot (4,2,0,0,1)$$
$$(6,1,2,0,0) = \frac{1}{2} \cdot (6,2,0,0,0) + 1 \cdot (3,0,2,0,0)$$

This shows that the constraints T8 and T9 are redundant, and the empirical constraints form a more strict set of restrictions. On the other hand, the empirical constraints are linearly independent given they are the facets of a convex hull. We have therefore encountered a similar situation as in the 5-pole case: The theoretical constraints are not tight due to the supposed existence of more strict empirical constraints.

Like in the 5-pole case, if we consider the boundaries compatible with the 6-cycle extension of G, the total number of flows with these boundaries must be positive, otherwise the extended G would form a planar snark. The boundaries compatible with the 6-cycle extension are 111111, 112332, 123123, and 111122. In contrast to the 5-pole case, there is one boundary that contains only a single color, thus we cannot ignore the color permutation. The total number of flows with the given boundaries (also taking the color permutation into account) is therefore equal to

$$x = 3 \cdot f^{\circlearrowleft}_{111111}(G) + 6 \cdot f^{\circlearrowleft}_{112332}(G) + 6 \cdot f^{\circlearrowleft}_{123123}(G) + 6 \cdot f^{\circlearrowleft}_{111122}(G) =$$
$$= 63a + 33b + 12c + 21d + 21e.$$

We can calculate the total number of flows in G in a similar manner, which gives us the value $t = 183a + 63b + 36c + 27d + 27e$. Analogously to the result for 5-poles, where

the empirical constraint implies that the number of flows compatible with the 5-cycle extension is at least a quarter of the total number of flows, the empirical constraints E1 and E9 for 6-poles imply that the number of flows compatible with the 6-cycle extension is at least one-eighth of the total number of flows. Specifically, if the empirical constraint E9 really holds, we get

$$\begin{aligned} 0 \leq 81 \cdot (a+b+d+e) + 60 \cdot (4a+2b+c+d+e) = \\ = 321a + 201b + 60c + 141d + 141e, \end{aligned}$$

which can be reorganized to

$$\begin{aligned} 504a + 264b + 96c + 168d + 168e &\geq 183a + 63b + 36c + 27d + 27e \\ 8 \cdot (63a + 33b + 12c + 21d + 21e) &\geq 183a + 63b + 36c + 27d + 27e \\ x &\geq \frac{1}{8}t, \end{aligned}$$

as desired. This indicates that for $k \geq 6$, we could formulate similar hypotheses for the flows compatible with different extension shapes. We could also attempt to use the 5-pole hypothesis directly to derive more inequalities about 6-poles by connecting two outer edges of a 6-pole G and stating the 5-pole hypothesis for the resulting 5-pole in terms of the coefficients of G. This however requires using all the 15 coefficients, since the relation is not symmetric under rotation and the reduced dimensions are thus not sufficient. This direction of research quickly becomes tedious and impractical, but a systematic search might yield insight into the relationship between the theoretical and empirical constraints for k-poles with different values of k.

Finally, we also computed the reduced coefficients of the $1.3 \cdot 10^{10}$ 7-poles for $v \leq 34$. Unfortunately, the growing dimensionality makes even such a large number of 7-poles insufficient to reliably conclude on the empirical constraints.

Conclusion

In this thesis, we studied the properties of the multipole polynomial coefficients over the group $(\mathbb{Z}_2 \times \mathbb{Z}_2, +)$. We described the connection between the Four color theorem and flows in cubic planar multipoles and used the multipole polynomial coefficients to study the properties of multipoles.

Our research shows that the multipole polynomial coefficients are powerful enough to capture non-trivial structural properties of planar multipoles: If we rely on the Four color theorem, it is possible to determine the connectedness and 2-connectedness of multipole parts solely from its coefficient values. If we omit the Four color theorem assumption, this result becomes an equivalent way of stating the Four color theorem itself.

We also demonstrated that the coefficients can be practically computed for small multipoles quickly despite the exponential nature of the computation. We devised an improved algorithm for this purpose and implemented features that make it more efficient also for multipoles that are not planar and cubic. When utilizing a computer with many CPU cores, it is possible to compute the coefficients of all cubic planar multipoles with up to approximately 30 vertices in the order of hours.

We analyzed the coefficient values for 4-, 5-, and 6-poles. In the case of 4-poles, the values behave as expected—they tightly satisfy the theoretical constraints given by the non-negativeness of the numbers of flows with a given boundary. However, in the case of 5-poles and 6-poles, the coefficient values appear to be more restricted than the theoretical constraints suggest. We formulated a hypothesis about the observed constraint for 5-poles and also restated it in terms of coloring counts: We hypothesize that for each cubic planar 5-pole, the colorings of the type `11123` represent at least one-quarter of the total number of colorings. We also showed that if the hypothesis is false, the smallest counterexample must be connected, contain no bridge or 2-cut (except the pairs of edges adjacent to the same dangling edge), and have at least 36 vertices.

The multipole polynomial coefficients thus proved to be a useful tool for studying the properties of planar multipoles. In the future, it would be interesting to attempt to prove the 5-pole hypothesis and to explore the empirical constraints systematically, as they seem to exhibit intricate connections to each other and the Four color theorem.

Bibliography

[1] Reinhard Diestel. *Graph theory*. Number 173 in Graduate texts in mathematics. Springer, 3rd edition, 2005. OCLC: ocm61167989.

[2] William T. Tutte. A Contribution to the Theory of Chromatic Polynomials. *Canadian Journal of Mathematics*, 6:80–91, 1954.

[3] William T. Tutte. Graph polynomials. *Advances in Applied Mathematics*, 32(1-2):5–9, January 2004.

[4] Martin Kochol. Reduction of the 5-Flow Conjecture to cyclically 6-edge-connected snarks. *Journal of Combinatorial Theory, Series B*, 90(1):139–145, January 2004.

[5] Martin Kochol. Decomposition formulas for the flow polynomial. *European Journal of Combinatorics*, 26(7):1086–1093, October 2005.

[6] Martin Kochol. Restrictions On Smallest Counterexamples To The 5-Flow Conjecture. *Combinatorica*, 26(1):83–89, February 2006.

[7] Martin Kochol. Smallest counterexample to the 5-flow conjecture has girth at least eleven. *Journal of Combinatorial Theory, Series B*, 100(4):381–389, July 2010.

[8] Matt DeVos. Flows on Bidirected Graphs, October 2013. arXiv:1310.8406 [math].

[9] G. D. Birkhoff and D. C. Lewis. Chromatic polynomials. *Transactions of the American Mathematical Society*, 60(0):355–451, 1946.

[10] W.T. Tutte. On the Birkhoff-Lewis equations. *Discrete Mathematics*, 92(1-3):417–425, November 1991.

[11] OEIS Foundation Inc. Coloring a circuit with 4 colors, Entry A006342 in The On-Line Encyclopedia of Integer Sequences, 2024. `https://oeis.org/A006342`.

[12] Frank Bernhart. *Topics in Graph Theory Related to the Five Color Conjecture*. PhD thesis, Kansas State University, 1974.

[13] OEIS Foundation Inc. Riordan numbers, Entry A005043 in The On-Line Encyclopedia of Integer Sequences, 2024. `https://oeis.org/A005043`.

[14] William Y.C. Chen, Eva Y.P. Deng, and Laura L.M. Yang. Riordan paths and derangements. *Discrete Mathematics*, 308(11):2222–2227, June 2008.

[15] OEIS Foundation Inc. Set partitions without singletons, Entry A000296 in The On-Line Encyclopedia of Integer Sequences, 2024. `https://oeis.org/A000296`.

[16] Gunnar Brinkmann, Heidi Van den Camp, and Brendan McKay. plantri and fullgen. Available online at `https://users.cecs.anu.edu.au/~bdm/plantri/` (retrieved April 16, 2024).

Appendix A

Source code and computed data

The electronic attachment contains the source code of the `C++` implementation of the coefficient computation algorithms described in Chapter 4, as well as the computed values for small cubic planar multipoles. The code used to analyze the data is located in the `analysis.ipynb` SageMath Jupyter notebook, which is also rendered in the HTML format for easier viewing in the `analysis.html` file. The contents of the attachment are also published on `https://github.com/davidmisiak/flow-polynomials`.